Journal of Hydrology 660 (2025) 133469

Contents lists available at ScienceDirect

Journal of Hydrology

journal homepage: www.elsevier.com/locate/jhydrol

Research papers

Controls on preferential flow and its role on streamflow generation in a Mediterranean forested catchment

K. Kaffas [a,b,*], I. Murgia [a], A. Menapace [c], M. Macchioli Grande [d], M. Verdone [a,e], A. Dani [a], F.S. Manca di Villahermosa [a], F. Preti [a], C. Segura [f], C. Massari [e], J. Klaus [g], M. Borga [h], D. Penna [a,e,f]

[a] Department of Agriculture, Food, Environment and Forestry, University of Florence, Florence, Italy
[b] Department of Science, Roma Tre University, Rome, Italy
[c] Institute for Renewable Energy, Eurac Research, Bolzano, Italy
[d] Department of Geology, Faculty of Physical and Mathematical Sciences, University of Chile, Santiago, Chile
[e] Research Institute of the Geo–Hydrological Protection, National Research Council, Perugia, Italy
[f] Forest Engineering Resources and Management Department, Oregon State University, Corvallis, USA
[g] Department of Geography, University of Bonn, Bonn, Germany
[h] Department of Land, Environment, Agriculture and Forestry, University of Padova, Padova, Italy

ARTICLE INFO

This manuscript was handled by Renato Morbidelli, Editor-in-Chief, with the assistance of Wei Hu, Associate Editor

Keywords:
Soil moisture
Matrix flow
Sequential response
Non-sequential response
Hillslope hydrology
Forested catchment
Hydrological response

ABSTRACT

The driving mechanisms of preferential flow in soils of Mediterranean forested catchments remain largely unexplored. We used soil moisture sensors to investigate these mechanisms along two hillslope transects in the Re della Pietra catchment (2 km^2) in the Tuscan Apennines, central Italy, to understand the drivers of preferential flow and its effect on streamflow generation. The study area has a temperate Mediterranean climate, consists of sandy-loam soils, and is covered almost entirely by a dense deciduous forest. We defined dry and wet periods using an automatic method based on the soil moisture signal's high and low envelope, considering field capacity and potential evapotranspiration thresholds. Among various hydrometeorological, topographic, and soil physical properties, antecedent soil moisture emerged as the primary driver of preferential flow at one hillslope, while dry bulk density dominated at the other hillslope. A supervised classification random forest model was highly effective in classifying the type of soil moisture response based on its timing and identifying the controlling factors. Precipitation events in the headwater subcatchments hosting one of the two hillslopes were classified according to the timing of soil moisture response leading to the identification of three distinct types of hydrographs, revealing the role of preferential flow on sustaining streamflow. Our results shed new light on preferential flow controls and their role in runoff generation, emphasizing the importance of these processes in seasonally dry and wet hydrologic systems, such as Mediterranean catchments, and the need to better understand their spatiotemporal patterns.

1. Introduction

Preferential flow (PF) has a substantial impact on catchments both in quantitative terms, i.e., promoting the infiltration of stormwater through accelerate flow pathways (Wang et al., 2023), contributing to groundwater recharge, and sustaining baseflow and stream runoff (Worthington, 2019; Zhang et al., 2018), and in qualitative terms, facilitating the transport of nutrients and contaminants through the soil and to the stream (Clothier et al., 2008; Franklin et al., 2021). PF occurs through macropores and other heterogeneous structures in the soil, including cracks and voids created by plant roots or pedofauna (Allaire et al., 2009; Beven and Germann, 1982; Grant et al., 2019; Guo et al., 2019; Zehe and Flühler, 2001), or as lateral flow along a hydraulically restrictive sloping layer, such as bedrock (Buttle and McDonald, 2002; Weiler and McDonnell, 2007). PF is characterized by rapid movement through preferred pathways (e.g., vertical and lateral flow, macropore, fingering, funnel, or unstable flow) predominantly driven by gravity and little influenced by capillarity. These features facilitate vertical and

* Corresponding author at: Department of Agriculture, Food, Environment and Forestry, University of Florence, Florence, Italy; Department of Science, Roma Tre University, Rome, Italy.
E-mail address: konstantinos.kaffas@uniroma3.it (K. Kaffas).

https://doi.org/10.1016/j.jhydrol.2025.133469
Received 15 January 2025; Received in revised form 27 April 2025; Accepted 5 May 2025
Available online 11 May 2025

lateral soil water redistribution through hydraulically connected networks and enhanced soil saturation (Sidle et al., 2001). The activation of PF networks on hillslopes often leads to the development of the hillslope-stream subsurface hydrological connectivity which typically plays a major role on catchment streamflow generation, especially during wet periods (Blume and van Meerveld, 2015; Penna et al., 2015; Von Freyberg et al., 2014).

Several studies argue that PF is mainly influenced by the amount and intensity of precipitation, antecedent soil moisture conditions, soil properties, and hillslope topography (Sidle et al., 2000, 1995; Tromp-Van Meerveld and McDonnell, 2006; Tsuboyama et al., 1994; Uchida et al., 2005). Precipitation intensity and amount primarily influence PF activation and magnitude (Flury et al., 1994; Wiekenkamp et al., 2016), while precipitation event duration is a secondary factor (Heppell et al., 2002). Additionally, soil matrix can rapidly absorb rainwater from low-intensity events, while intense events favor PF (Beven and Germann, 1982; Heppell et al., 2002). High-intensity or long-duration precipitation events can cause PF-induced rising subsurface storm flows (Beven and Germann, 2013; Nieber and Sidle, 2010), leading to high peak flows and enhanced flow rates and volumes (Uchida et al., 2001). Conversely, some studies show that increased intensities (Radolinski et al., 2021; Wu et al., 2015) and raindrop impact (Assouline and Ben-Hur, 2006) reduce PF. Nevertheless, evidence indicates that such precipitation characteristics did not significantly influence PF in Mediterranean catchments, where soil moisture is the predominant factor (Nanda and Safeeq, 2023). Antecedent soil moisture emerges as another critical controlling factor in PF generation in natural (Ali et al., 2015; Detty and McGuire, 2010; Tromp-Van Meerveld and McDonnell, 2006) and agricultural (Cain et al., 2022; Lam et al., 2016; Williams et al., 2019; Williams and McAfee, 2021) landscapes. Soil moisture changes can affect PF by altering the pore network (e.g., desiccation cracks produced in highly clayey soils; Greve et al., 2012) and matrix-macropore interactions (e.g., inducing hydrophobicity; Jarvis et al., 2016), or promoting the saturation of soil layers (Cain et al., 2022; Williams and McAfee, 2021). Once the soil reaches field capacity, gravity promotes water movement, generating PF (Song and Wang, 2019). Additionally, PF frequency peaks during dry seasons (Nanda and Safeeq, 2023; Tang et al., 2020), with dry conditions also initiating PF (Hardie et al., 2011; Lin and Zhou, 2008; Liu and Lin, 2015; Nanda and Safeeq, 2023; Tang et al., 2020), amplifying soil moisture gradients, and enhancing cumulative infiltration. However, Wiekenkamp et al. (2016) observed that soil moisture did not significantly impact PF in a temperate forest catchment but was strongly influenced by the interaction among soil structure, precipitation characteristics, and catchment-specific factors. Soil structure influences PF through continuity, tortuosity, and hydraulic connectivity. Soil heterogeneities such as macropores, pipes, cracks, and textural discontinuities promote water infiltration into deeper soil layers (e.g., Guo and Lin, 2018; Jarvis, 2007) and lateral flow development (Noguchi et al., 1999). Regarding soil texture, coarser soils experience finger-flow PF due to hydraulic instability, while finer soils are mostly characterized by a macropore control (Hangen et al., 2005; Mooney and Morris, 2008). Specifically, clay content significantly influences PF initiation in undisturbed conditions (Koestel and Jorda, 2014; Liu and Lin, 2015). Soil hydraulic properties like conductivity and water retention are essential for PF initiation, influenced by small-scale heterogeneity and gradient changes (Gazis and Feng, 2004; Hangen et al., 2005; Köhne et al., 2006; Kulasekera et al., 2011). Hydrophobicity from organic matter decomposition hinders soil wetting and impacts PF velocity and water inlet (Bauters et al., 1998; Dekker and Ritsema, 1994). Finally, topography represents another critical factor influencing the initiation of PF. In general, steep slopes facilitate PF more effectively than planar sites due to steeper hydraulic gradients and higher subsurface flow rates typically observed in such landscapes than in flatter regions (Liu and Lin, 2015; Singh et al., 2021). Investigations on PF initiation at various hillslope positions demonstrated that PF primarily occurs at the lowest hillslope locations (Dymond et al., 2021; Nanda and Safeeq, 2023) due to increased soil moisture values.

Various methods can be used to assess PF controls, including field experiments with tracers, infiltrometers, soil moisture probes, and advanced geophysical techniques. In hydrological research, machine learning is emerging as a viable alternative to physical models because of its simplicity (Solomatine and Ostfeld, 2008). Recent studies have utilized machine learning techniques for probabilistic forecasting, particularly concerning the occurrence of floods (Papacharalampous and Tyralis, 2022) and sediment transport (Desai and Ouarda, 2021; Schoppa et al., 2020), as well as the downscaling of soil hydrological mapping (Gagkas and Lilly, 2019) and the estimation of root zone soil moisture (Carranza et al., 2021). Deep learning approaches have also been used to extract PF characteristics from dye-tracing images. For instance, the recent work of Bai et al. (2023) applied a dual-scale attention residual UNet (DARM-UNet) architecture to accurately segment PF features in forest soils, outperforming traditional image processing and deep learning methods. Random Forest (RF) algorithms are specifically applied to identify the best predictors of the investigated phenomenon. Soil susceptibility to PF was estimated through RF predictions based on a literature database (Koestel and Jorda, 2014), while other works studied the relation between PF and soil properties, such as hydraulic connectivity and soil moisture (Kang et al., 2023; Zhang et al., 2024) or snowpack development (Avanzi et al., 2019).

The analysis of the aforementioned studies points out that multiple factors, such as precipitation characteristics and antecedent soil moisture conditions, control PF initiation but they often act differently according to local conditions, mainly due to the complex nature of the phenomenon. Particularly, the dynamics of PF in Mediterranean mountain forested catchments and their effect on streamflow generation remain largely uncharted and necessitate further investigation. Our study makes a decisive contribution to filling this gap by utilizing three years of hydrometeorological, topographic, and soil data collected from the Re della Pietra experimental catchment to investigate the dynamics of PF in Mediterranean mountain forested catchments and its role in streamflow generation, an area that remains largely unexplored. Moreover, RF algorithms to identify the principal drivers of PF in seasonally wet and dry Mediterranean catchments have not yet been applied. RF was selected for its strong performance in classification tasks, particularly its ability to capture complex, nonlinear interactions between variables, handle high-dimensional data, and provide internal feature importance metrics. Our study is the first-ever to apply RF for predicting the occurrence of PF and the impact of its controlling factors in Europe or the Mediterranean region. To date, only two known examples exist where RF has been applied in this context: Kocian and Mohanty (2024) used RF to examine both the occurrence and controls of PF at a large scale across the Continental United States, and Kang et al. (2023) focused on the controls of PF in Northwest China. This makes our application uniquely novel at the European scale, and especially for the Mediterranean setting, but also globally significant given that only two other studies have applied RF in a similar context (Kang et al., 2023; Zhang et al., 2024). Therefore, in this study we rely on three years of hydrometeorological data collected in the Re della Pietra experimental catchment (central Italy) to investigate the role of hydrometeorological, topographic, and soil factors on PF initiation. By leveraging both field data and RF, this work aims to disentangle the complex interplay of factors driving PF initiation in Mediterranean forested catchments. Specifically, we addressed the following research questions:

i) How do precipitation characteristics, antecedent conditions, soil properties, and hillslope topography control PF initiation during dry and wet periods?
ii) How does PF impact streamflow generation?

2. Materials and methods

2.1. Study area

The Re della Pietra (RdP) is a small experimental forested catchment (2 km^2) in the Tuscan Apennines, in central Italy (Fig. 1). The catchment is instrumented to monitor ecohydrological variables including meteorological parameters, stream stage and streamflow, and volumetric soil moisture, among others, across different spatial scales, from the outlet of the RdP up to one of its headwater sub-catchments, Lecciona (0.31 km^2). Except for a small forest road network that occupies less than 5 % of the area, the catchment is covered entirely by dense forest, mainly composed of beech and oak trees, and planted conifers (*Fagus sylvatica, Quercus cerris, Pseudotsuga menziesii and Pinus nigra*) that determine canopy interception up to 25 % (Verdone et al., 2025). The climate is temperate Mediterranean characterized by mean annual precipitation of 1300 mm and mean air temperature of 10.5 °C with a monthly range between 2 °C and 20 °C, based on data from a weather station situated at 955 m a.s.l., 12 km south of the catchment area and operated by the Regional Hydrological Service. The terrain is mountainous, with steep hillslopes (mean slope of 27.5°) and elevation ranges between 634 m and 1320 m a.s.l., with a mean elevation of 1006 m. Soil texture is sandy, with all samples classified as sandy loam, while the geological composition of the catchment comprises sandstones from the Miocene Macigno Formation, dating back to the Late Oligocene to Early Miocene period (Amendola et al., 2016).

2.2. Equipment and dataset

In this study, we used precipitation, soil moisture, and streamflow data. Precipitation depth was recorded every 5-min, with a tipping bucket rain gauge that was dynamically calibrated (Marsalek, 1981; Sypka, 2019) also considering the possible effect of wind undercatch (Hosking et al., 1985; Rinehart, 1983), by a weather station installed in an open area on the southwest boundary of the Lecciona sub-catchment and by a rain gauge at C4, the outlet of the RdP catchment (Fig. 1). Two sets of six soil moisture sensors were installed along two hillslope transects (henceforth, also referred to as sites), one in the Lecciona sub-catchment and one a few hundred meters upstream C4 (Fig. 1). The two sites and their corresponding data are henceforth also referred to as Lecciona and C4, respectively. Each set of soil moisture probes was placed in pairs, at 15 cm and 35 cm depths (referred to as shallow and deep layer, respectively), at three topographic positions along a hillslope gradient. In Lecciona, all three sensors are positioned in the lower and middle part of the hillslope. The positions are referred to as riparian, footslope, and midslope, reflecting their relative placement within this lower section (Fabiani et al., 2024; Macchioli Grande et al., 2024). Canopy cover at the three hillslope positions was assessed using Sentinel-2 Leaf Area Index (LAI) values, which indicated a dense canopy across all positions. The recorded LAI values, derived as a median during the first half of summer (15 June-15 July), were 2.87, 2.98, and 2.81 for the riparian, footslope, and midslope positions, respectively. This suggests that the canopy cover is continuous and substantial, typical of a mature forest. The summer period (15 June–15 July) was specifically

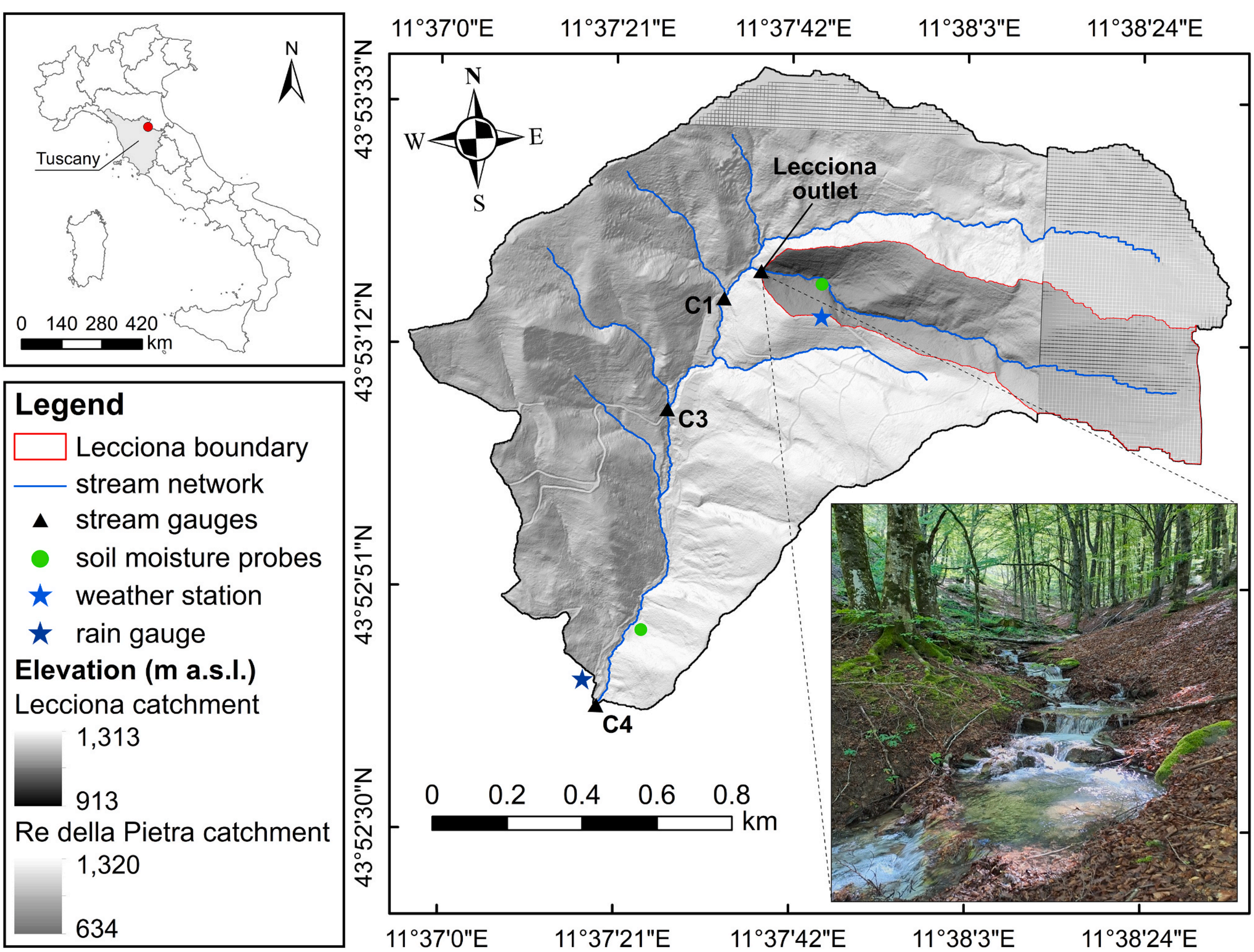

Fig. 1. Map and picture of the study area and, in the upper-left corner, its position in the country.

chosen for this analysis, as it corresponds to the time when the deciduous trees are in full leaf, therefore representing the maximum canopy cover. In C4, all three sensors are also located in the lower part of the hillslope but are situated further from the riparian zone. The positions are referred to as bottom, middle, and top, indicating their relative placement with respect to each other within this section of the slope (Fig. 2). Soil moisture raw values were converted into volumetric water content (m^3/m^3) by applying a standard calibration for mineral soils suggested by the manufacturer (Macchioli Grande et al., 2024). The probes recorded at a 10-min time step over a period of 34 months (August 2020 – May 2023) in Lecciona and 18 months (December 2021 – May 2023) in C4. Stream stage was monitored at 10-minute intervals using a CTD (Conductivity, Temperature, Depth) sensor, with measurement precisions of ± 0.05 % mm for water level. A composite rectangular-triangular weir coupled with a pressure transducer at the Lecciona outlet enabled the stage-streamflow conversion at Lecciona (Macchioli Grande et al., 2024).

2.3. Identification of preferential flow events

We identified the occurrence of PF based on the different response time of the deep and the shallow soil moisture probes to precipitation events, following the approach outlined by Lin and Zhou (2008) and subsequently adopted by studies such as Graham and Lin (2011), Hopkins et al. (2016), and Tang et al. (2020). According to this approach, a first soil moisture response at the shallow layer is defined as sequential response (mainly driven by matrix flow), while a first response at the deeper layer is defined as non-sequential response and suggests the occurrence of PF (Fig. 3).

Precipitation events were defined as at least 1 mm of precipitation and a minimum inter-event time (MIT) of 4 h with no precipitation. Precipitation records from the rain gauge at the RdP outlet were employed for analyzing soil moisture data at C4, while precipitation data from the weather station were used for analyzing soil moisture measured at Lecciona.

For each probe, we defined the soil moisture response to precipitation events as a ≥ 1 % increase in soil moisture content after a precipitation input compared to the antecedent soil moisture (ASM) (Graham and Lin, 2011; Tang et al., 2020; Wiekenkamp et al., 2016) (Eq. (1). We considered ASM as the average soil moisture of the three time steps (namely, 30 min) prior to the soil moisture response.

$$if\begin{cases} \theta_t \geq thresh, Response \\ \theta_t < thresh, NoResponse \end{cases} \quad (1)$$

where *thresh* is the threshold set, by definition, to mark a soil moisture response (m^3/m^3); and θ_t is the volumetric soil moisture at time t (m^3/m^3).

Taking into account the two types of responses presented in Fig. 3, we defined the following three soil moisture response types:

i) Sequential (SEQ) response: soil moisture responds earlier in the shallow soil layer, potentially followed by a subsequent response in the deeper layer.
ii) Non-sequential (non-SEQ) response: soil moisture responds earlier in the deep soil layer, potentially followed by a subsequent response in the shallow layer. This type of response indicates the occurrence of PF (Demand et al., 2019; Graham and Lin, 2011; Tang et al., 2020).
iii) No response: soil moisture at any depth does not exceed the 1 % increase.

A high variability of soil moisture was observed during the precipitation events, often resulting in multiple responses during the same event, meaning that the threshold (Eq. (1)) was exceeded multiple times

Fig. 2. Hillslopes with the middle positions, referred to as “footslope” for Lecciona (left) and “middle” for C4 (right), standing out with the data loggers on a stick. These pictures were taken from the riparian position in Lecciona and the bottom position in C4. The cables extend upslope to the other two positions at each site.

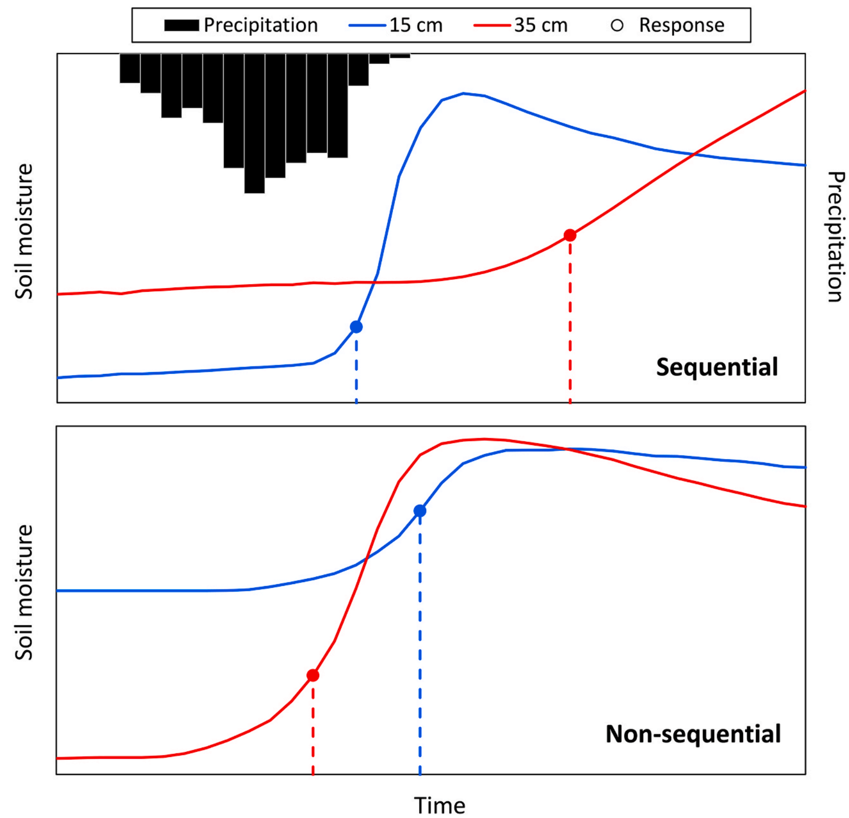

Fig. 3. Conceptual schematics of the soil moisture response types. The blue dots indicate the soil moisture response at the shallow layer, while the red dots represent responses in and deep layer. The vertical dahs lines mark the response timing for the shallow (blue) and the deep (red) layers. (For interpretation of the references to colour in this figure legend, the reader is referred to the web version of this article.)

during certain precipitation events. These multiple responses were taken into account and were treated as individual responses only when the monotony of the soil moisture curve changed, namely when the threshold was exceeded following a soil moisture decrease. In total, we identified 139 responses at Lecciona during the 34 months and 160 responses at C4 during the 18 months.

2.4. Precipitation event-based analysis

Precipitation characteristics (depth, duration, and maximum intensity) and antecedent moisture conditions were considered as possible controlling factors on soil moisture SEQ or non-SEQ response on the two hillslopes. ASM was computed through the Antecedent Soil moisture Index (ASI) according to Haga et al. (2005):

$$ASI = \theta \times D \tag{2}$$

where θ is the volumetric soil moisture content (m^3/m^3); and D is the depth of installation (mm).

The antecedent moisture θ in the case of ASI was calculated as the mean between the two probes at a given position, averaged over six time steps (60 min) before the start of a precipitation event. In addition, precipitation depth was summed to ASI (indicated as ASI + P) to consider the combination of these two factors on soil moisture response.

The effect of seasonality on soil moisture response was assessed by evaluating the response types separately during dry and wet periods. We defined dry and wet periods using an automatic methodology based on the difference between the high and low envelope of the soil moisture signal. Considering that this difference tends to zero during dry periods, we defined a range of values from −0.005 to + 0.005, for which we assumed dry conditions. However, because such processing produces "false dry periods" without prolonged precipitation during wet periods, we considered a threshold value of field capacity equal to 0.2 $m^3\ m^{-3}$, identified from literature for sandy soils (Gong et al., 2012). Therefore, if the previously identified dry period showed soil moisture values above the field capacity, we considered it to be wet. Finally, we considered potential evapotranspiration, using the Thornthwaite method (Thornthwaite, 1948), to improve the identification of the end and beginning dates of each period. In our study, we selected the deep probe (35 cm) at the top position in the Lecciona hillslope as a reference for identifying dry and wet periods. This choice was based on the time series length, which is longer for the Lecciona site, allowing us to identify dry and wet periods before monitoring in C4. Additionally, we selected the top-position probe to avoid the potential influence from stream proximity on soil moisture values.

The controlling factors were calculated each time with reference to the time step of the first soil moisture response for each pair of sensors (15 cm and 35 cm depth). Hence, precipitation depth, duration, and maximum intensity were considered from the start of the precipitation event until the first soil moisture response separately for each hillslope position.

2.5. Identification of preferential flow

A RF supervised classification algorithm (Breiman, 2001) was used to analyze and predict the occurrence of SEQ and non-SEQ soil moisture responses on the two study hillslopes. Apart from the antecedent moisture conditions and precipitation depth, duration, and maximum intensity, which are dynamic variables, i.e., changing for each soil moisture event, a set of time invariant predictors was tested as possible controls of soil moisture response. These comprise: i) the soil dry bulk density (kg/m^3) for each depth and hillslope position, ii) the local slope for each hillslope position (°), and iii) the Topographic Wetness Index (TWI) for each hillslope position. The local slope was computed through a LiDAR-derived Digital Elevation Model of the study catchment. TWI is an expression of the spatial scale effect on hydrological processes (Beven and Kirkby, 1979):

$$TWI = ln\frac{a}{tanb} \quad (3)$$

where α is the upslope contributing area (m^2); and b is the local slope (radians).

Though the effect of topography and drainage area on the variability of soil moisture is well-documented in the literature (Li et al., 2022; Nanda et al., 2019), we aimed to test whether time-invariant controls can contribute to the predictive power of the RF model. Additionally, we proposed the ratio of precipitation depth to local slope and TWI, namely P/slope and P/TWI, to convert these two parameters to dynamic variables. Thus, the effect of local slope and TWI on controlling the type of soil moisture response could also be assessed in addition to their time-constant counterparts and to precipitation itself, resulting in a total of twelve parameters (Table 1). While an explicit seasonality index was not included, soil moisture inherently captures seasonal variations, serving as a proxy for these effects in our analysis. The entire datasets for Lecciona and C4 are made available in Tables S1 and S2 in the Supplementary material Section.

A robust calibration procedure was employed to ascertain the optimal random forest model for effectively conducting sensitivity analysis of the different factors related to the soil moisture response. Specifically, the model was trained using 70 % of the data, while the remaining 30 % was reserved for testing, adhering to a 70–30 split ratio (Nguyen et al., 2021). The random forest algorithm was implemented in R. One hundred datasets were created by randomly selecting training and testing data while maintaining a fixed split ratio. For each generated dataset, the training was repeated using models with one to twelve features, resulting in 12 different models per dataset and a total of 1200 models. This robust procedure allowed for the selection of the best-performing model in terms of both the number of features (controlling factors) and the effective number of trees.

Specifically, the number of features randomly sampled as candidates at each split was evaluated across 100 datasets using two metrics: i) the out-of-bag error (OOB), which provides an internal estimate of the generalization error, and ii) the mean absolute percentage error (MAPE) in prediction, which provides the accuracy of the model on new data in terms of percentage of wrong predictions in the testing period. The best model was subsequently selected using the Euclidean distance of the two standardized metrics (0–1) based on the following relationship:

$$finalrank = \sqrt{OOB\_sd^2 + MAPE\_sd^2} \quad (4)$$

where OOB_sd and $MAPE\_sd$ are the standardized OOB and MAPE, respectively.

The model with the highest predictive power ("best" model) was the one with the lowest value of the final rank.

On the other hand, while analyzing the effect of different numbers of features, the effective number of trees was also investigated. Specifically, each model was trained with a fixed upper limit of 300 trees to ensure sufficient learning capacity, and for each repetition, the number of trees corresponding to the minimum out-of-bag (OOB) error was recorded. This enabled the identification of the minimum number of trees required for each feature set, ensuring optimal model performance while avoiding unnecessary complexity, simulation time and computational costs. To enhance robustness against noise and variability, the final number of trees was defined as the 75th percentile of the distribution of optimal tree counts across all runs, ensuring a balance between accuracy, efficiency, and generalization.

The optimum number of features and trees was selected based on this multi-criteria ranking, which ensures both internal generalization and predictive accuracy in identifying the best model. This strategy also helps mitigate overfitting by favoring parsimonious models with fewer features, leveraging repeated validation across multiple datasets, and avoiding overly complex trees through the selection of optimal tree counts. Thus, despite common limitations of random forest models, such as reduced interpretability, sensitivity to noisy data, and the need for sufficient training samples, these were effectively addressed through the proposed rigorous calibration and validation approach. Moreover, random forest remains well-suited for this application due to its ability to handle nonlinear relationships, capture feature interactions, and provide internal performance metrics and variable importance measures, which aligns closely with the primary goal of the proposed study.

Then, the best model was first used to analyze the most significant features, using the Mean Decrease Accuracy (MDA) and Mean Decrease Gini Index (MDGI), and second to predict the SEQ and non-SEQ soil moisture responses. The MDA measures the impact of each variable on the model's accuracy by permuting the values of that variable and observing the resulting change in accuracy. Like MDA, and in contrast with the traditional Gini coefficient, which is an index of statistical dispersion, MDGI quantifies the importance of a feature in classifying a target variable. The Gini index itself is a measure of impurity or inequality in a dataset, used in decision trees to determine splits. Higher MDA and MDGI values indicate that permuting the variable's values leads to a greater decrease in model accuracy, suggesting that the variable is more important in the model's classification. Due to the stochastic nature of random forests and potential noise in the data, extremely small or negative MDA values might occur unlike MDGI, which is never negative. These values are often negligible and are more likely to be artifacts of the randomization process rather than meaningful insights into variable importance. A negative MDA value implies that permuting the variable's values somehow improves the model's accuracy, which is counterintuitive, but still highlights the lack of influence.

Table 1
Potential controlling factors on soil moisture response for the random forest application.

Factor (and unit of measurement)	Description
Precipitation (mm)	Precipitation depth from the beginning of the precipitation event until the soil moisture response
Duration (min)	Precipitation duration from the beginning of the precipitation event until the soil moisture response
Average precipitation intensity (mm/hr)	Average precipitation intensity from the beginning of the precipitation event until the soil moisture response
Maximum precipitation intensity (mm/hr)	Maximum precipitation intensity from the beginning of the precipitation event until the soil moisture response
ASI (mm)	Antecedent soil moisture index
ASI + P (mm)	Antecedent soil moisture index + precipitation depth
TWI (–)	Topographic wetness index
Precipitation/TWI (–)	Precipitation depth/TWI
Slope (°)	Local slope
Precipitation/slope (–)	Ratio between precipitation depth and local slope
Dry bulk density 15 cm (kg/m^3)	Dry bulk density in the shallow layer
Dry bulk density 35 cm (kg/m^3)	Dry bulk density in the deep layer

2.6. Preferential flow as control of catchment hydrological response

We assessed the role of the type of soil moisture response and of PF on streamflow generation in the Lecciona sub-catchment, where streamflow data were available. We considered only precipitation events which triggered both soil moisture and streamflow responses (Macchioli Grande et al., 2024). In addition to soil moisture events characterized by SEQ or non-SEQ responses only, some events led to both SEQ and non-SEQ responses across the three hillslope positions.

While the soil moisture analysis was based on distinguishing only between SEQ and non-SEQ responses, and each response was treated as an individual event, this was not possible in this case, as hydrographs refer to the entire precipitation event. Since there were precipitation events with only SEQ, non-SEQ, or a mixture of both responses along the hillslope, the following classification was adopted to investigate the effect of the soil moisture response type on streamflow generation:

i) SEQ: precipitation events which led to SEQ soil moisture responses only.
ii) Non-SEQ: precipitation events which led to non-SEQ soil moisture responses only.
iii) Mixed: precipitation events during which both SEQ and non-SEQ soil moisture responses occurred across the hillslope.

To facilitate the comparison among the three classes, all hydrographs were normalized by their peak discharge and averaged to a single mean normalized hydrograph for each of the above classes. Time was also normalized by the entire duration of each hydrograph.

In summary, we have monitored soil moisture responses to precipitation events, recorded at a 10-minute interval, across two hillslope transects, classifying them into sequential and non-sequential (PF) responses. A Random Forest model was used to evaluate the influence of meteorological, topographic, soil and hydrological controls on soil moisture response, while streamflow data from the Lecciona subcatchment were analyzed to assess the role of preferential flow in catchment hydrological response. The following sections present the results, beginning with the spatio-temporal variability of soil moisture responses before examining their connection to hydrological processes at the catchment scale.

3. Results

3.1. Spatio-temporal variability of soil moisture responses

3.1.1. Soil moisture seasonality and proportion of response types

Soil moisture exhibited a marked variability across depths and positions. In Lecciona, three distinct soil moisture patterns emerged: a coupled 15 cm and 35 cm behavior at the midslope position, decoupled signals at the footslope position, and a coupled/decoupled dynamics during dry and wet periods, respectively, at the riparian position (Fig. 4, upper panel). At 15 cm, the footslope position consistently exhibited the lowest soil moisture, while at the 35 cm it maintained higher moisture than the other positions. Notably, non-SEQ responses dominated at the footslope and riparian positions during dry periods, with the midslope position being the most responsive overall.

In C4, soil moisture exhibited multiple responses during precipitation events along with a more uniform behavior across positions, and clear convergence during wet periods (Fig. 4, lower panel). At 35 cm, the top position maintained the highest soil moisture for most of the study period, whereas at 15 cm the bottom position consistently featured the lowest soil moisture. All probes at 15 cm were unresponsive after prolonged rainless periods, contrasting the 35 cm layer where soil moisture promptly reacted to precipitation after dry periods. Non-SEQ responses were frequent at the middle position, limited at the top position (unlike in Lecciona), and were consistent at the bottom position during dry periods.

Both non-SEQ and SEQ responses predominantly occurred during wet periods (Fig. 5), which aligns with the study's wet-dominated conditions (wet periods covered 26 of the 34 months; Fig. 4). Non-SEQ responses proportionally covered a larger part of the wet period than SEQ responses. At the top position in C4, all non-SEQ responses occurred during wet periods. This pattern was disrupted both at the riparian position in Lecciona and the bottom position in C4, where SEQ

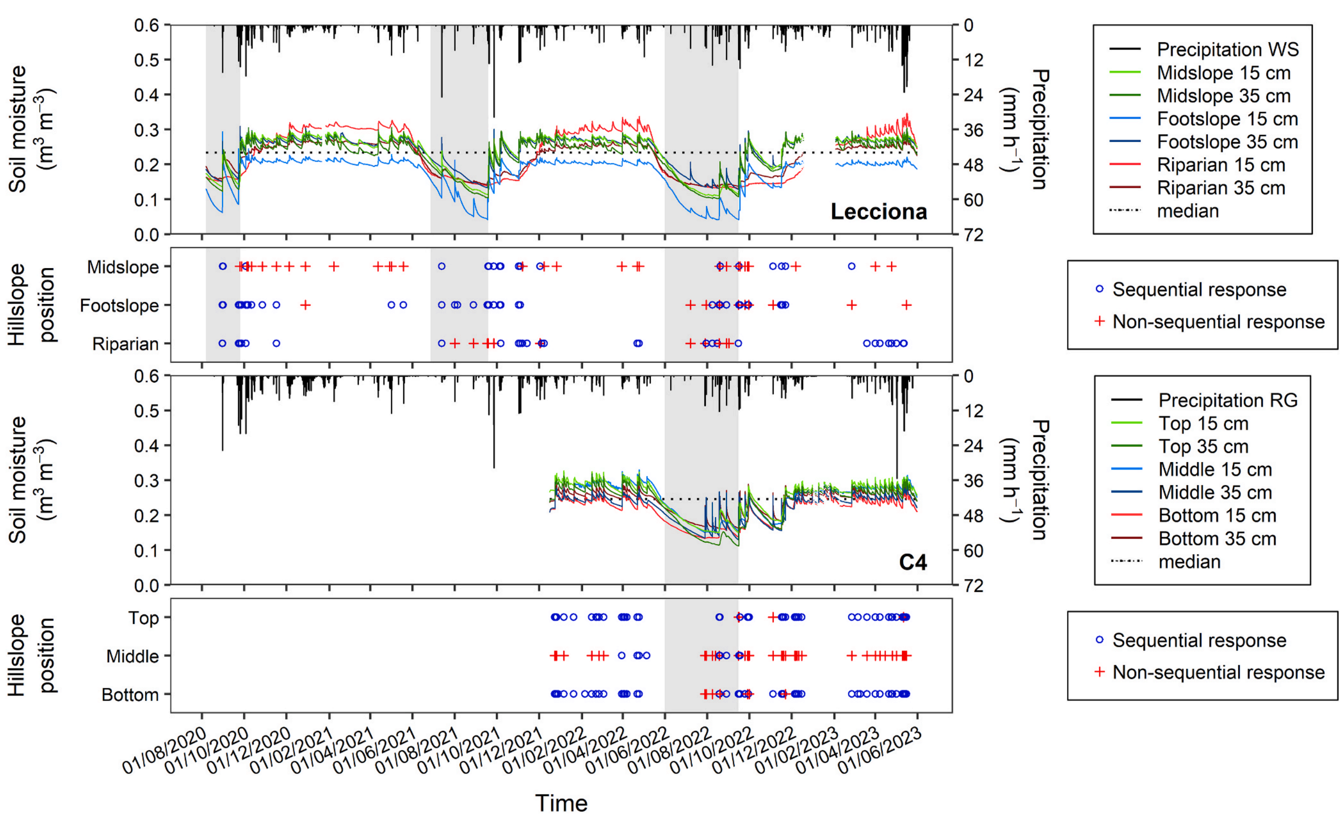

Fig. 4. Soil moisture seasonality and response types in Lecciona and C4. The gray shaded areas mark the dry periods defined by the envelope approach explained in Section 2.4.

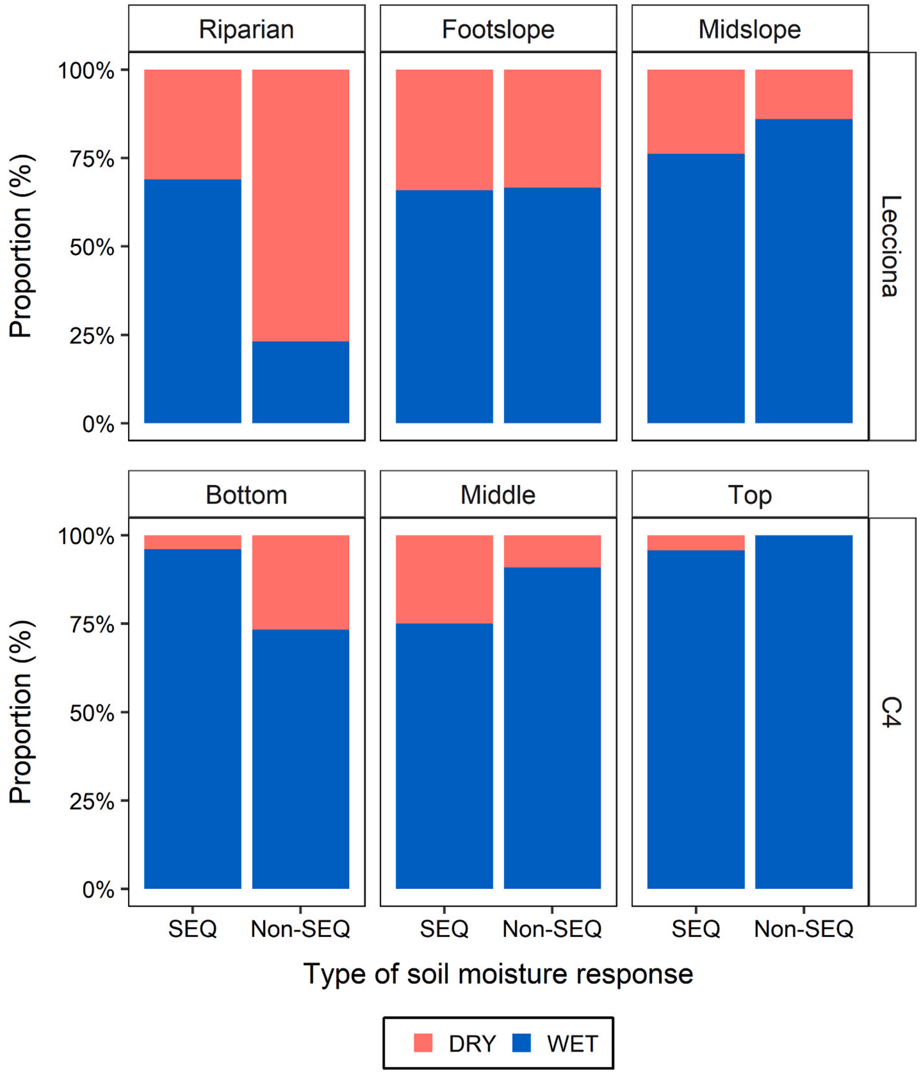

Fig. 5. Proportion of soil moisture response types at the two sites for wet and dry periods.

responses dominated the wet periods except in Lecciona, where most of the non-SEQ responses occurred during dry periods.

Though Fig. 5 accurately depicts the proportion of soil moisture response types in the two sites, it does not reflect the relative frequency of SEQ and non-SEQ response occurrences during wet and dry periods. The relative PF response frequency was calculated by the following relationship:

$$PF\% = \frac{Non\text{-}SEQresponses}{SEQresponses + Non\text{-}SEQresponses} * 100\% \tag{5}$$

where *PF%* is the relative frequency of non-SEQ responses defined by the fraction of the number of non-SEQ responses over the total number of soil moisture responses; *Non-SEQ* responses is the number of non-SEQ responses; and *SEQ* responses is the number of SEQ responses.

Most non-SEQ responses occurred during wet periods, and their relative frequency during the dry season in Lecciona was nearly equal to the wet season relative frequency. In C4, the non-SEQ relative frequency during the dry season was considerably higher than that one in the wet season (50.0 % against 29.6 %). Given the considerably fewer dry days and precipitation events during dry periods, the likelihood of PF under dry conditions is much higher than under wet conditions (Table 2).

3.1.2. Conditions associated with different types of soil moisture responses

Overall, in Lecciona, a high proportion of non-SEQ responses was

Table 2
Summary of soil moisture responses at the two sites for dry and wet periods.

	Lecciona				C4			
	Total Soil Moisture responses	**SEQ responses**	**Non-SEQ responses**	**Non-SEQ response relative frequency (%)**	**Total Soil Moisture responses**	**SEQ responses**	**Non-SEQ responses**	**Non-SEQ response relative frequency (%)**
Entire study period	139	87	52	37.4	160	109	51	31.9
Dry season	43	27	16	37.2	18	9	9	50.0
Wet season	96	60	36	37.5	142	100	42	29.6

associated with low precipitation depths, short durations, and low maximum intensity (Fig. 6). Despite some higher values, the bulk of non-SEQ responses occurred for lower values of all precipitation characteristics (Figs. 6a–c). This was more evident at the riparian and footslope positions, where there was a higher clustering of non-SEQ responses at the lower end of the values' range compared to the more dispersed SEQ responses. Moreover, non-SEQ responses were also associated with high or relatively high ASM conditions at all positions (Figs. 6d and e). This was particularly evident at the midslope position, where there was a clustering at the higher end of the ASI range, with a mean ASI of 88 mm (Fig. 6d). ASI + P had a smaller range compared to precipitation alone and non-SEQ responses occurred at higher values of ASI + P compared to SEQ responses (Fig. 6e). It is worth noticing that, with the exception of maximum precipitation intensity, all the examined parameters displayed the least dispersion for the occurrence of non-SEQ responses at the riparian position, showing a consistency regarding the hydrometeorological conditions that initiate PF.

In C4, neither precipitation characteristics (Figs. 7a–c) nor antecedent moisture conditions (Figs. 7d and e) seemed to have an evident control on PF. Similarly to Lecciona, non-SEQ responses occurred for relatively low values of precipitation characteristics and high antecedent moisture conditions, but comparison with the SEQ responses did not lead to coherent conclusions.

The results of the RF model confirmed the difference between the two sites (Fig. 8). In Lecciona, the MDA and MDGI were by far larger for ASI and ASI + P than for any other factor. This rendered the ASM conditions the most significant driver in discerning the soil moisture response type, exceedingly outweighing the other factors. The significance of precipitation depth in discerning the response type was considerably lower, and hence, its addition to ASI slightly weakened the significance of ASI + P, dropping the median MDA from 9.0 to 8.3. The third most dominant factor was precipitation duration, with a median MDA of 3.4 followed by TWI and dry bulk density at 15 cm, while the least significant was the maximum precipitation intensity, which was

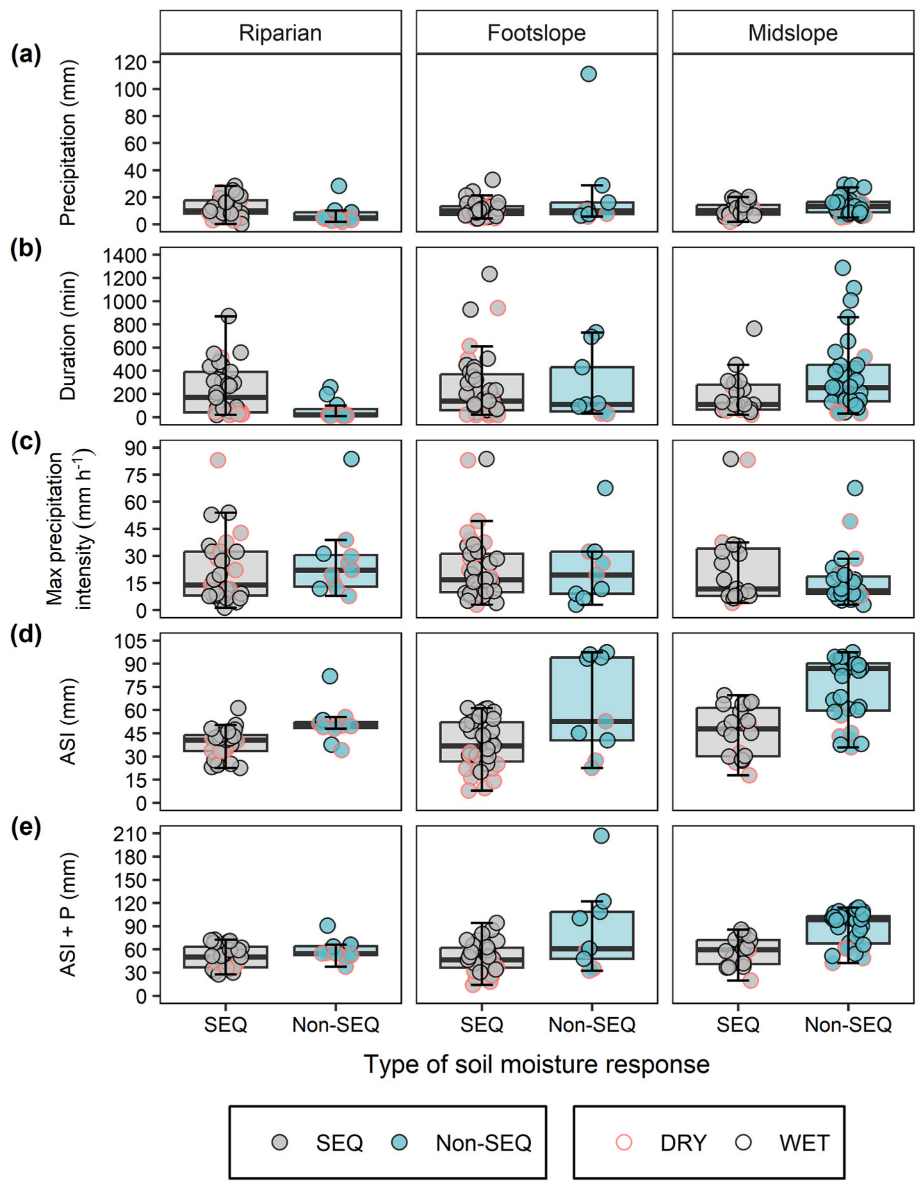

Fig. 6. Box-and-whisker plots with jitter point values of a) precipitation, b) duration of soil moisture event, c) maximum precipitation intensity, d) ASI, and e) ASI + P, by hillslope position and soil moisture response type in Lecciona. The boxes represent the first and third quartiles, the error bars represent the data within 1.5 times the interquartile range (IQR), and the black horizontal line marks the mean. The grey and light-green fillings indicate SEQ and non-SEQ soil moisture responses, respectively, whereas the red and black borders of the points indicate dry and wet periods. (For interpretation of the references to colour in this figure legend, the reader is referred to the web version of this article.)

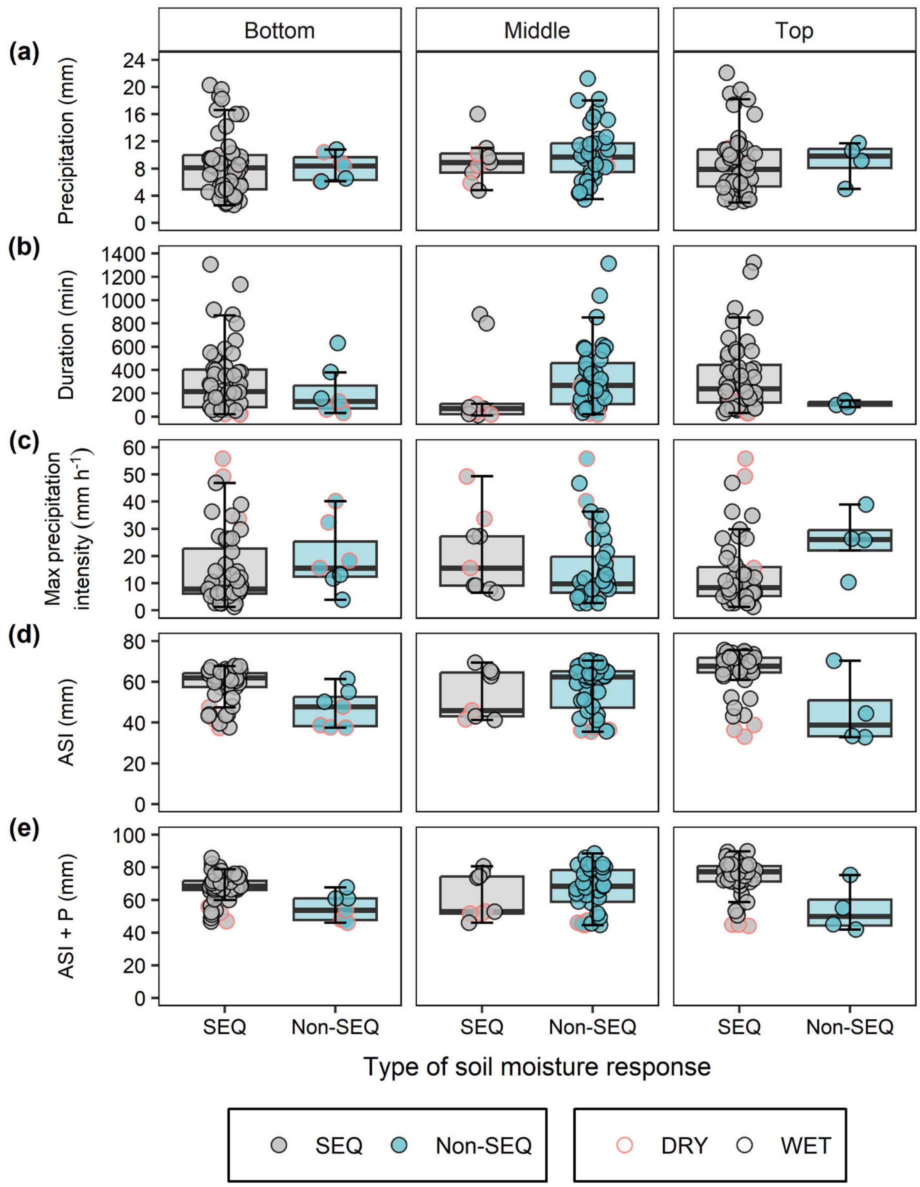

Fig. 7. Box-and-whisker plots with jitter point values of a) precipitation, b) duration of the soil moisture event, c) maximum precipitation intensity, d) ASI, and e) ASI + P, by hillslope position and soil moisture response type in C4. All other elements are represented as described in Fig. 6.

the only parameter with a median MDA close to zero (Fig. 8, upper panels).

MDA and MDGI produced different rankings, meaning that a parameter with high MDA did not necessarily contribute as much to reducing the Gini impurity index and, hence, effectively separating the classes of the target variable within the decision tree nodes. For example, TWI had higher MDA but lower MDGI than precipitation depth. Seemingly, one of the weakest parameters is the dry bulk density at 35 cm, which had both MDA and MDGI < 1, unlike the dry bulk density of the shallow layer, which was a stronger driver. The role of slope as a controlling factor was also negligible. The dynamic version of slope, i.e., precipitation/slope, improved its MDA, amplifying the effect of topography. However, this was not the case for precipitation/TWI, which displayed lower MDA, but higher MDGI, compared to TWI.

In C4, dry bulk density at both depths controlled the type of soil moisture response more than any other factor (Fig. 8 lower panels), with the shallow layer exerting slightly higher influence than the deeper layer with median MDA 5.8 over 5.7 of the deep layer. The third most significant factor in Lecciona, −the duration was not important in C4. The same stands for all precipitation characteristics, including precipitation depth and maximum precipitation intensity, which were not robust drivers. Topography played a more decisive role in C4 compared to Lecciona. It should be mentioned that local slope discrepancies along the hillslope transect were not great in the two sites, in contrast with the drainage areas, which for riparian, footslope, and midslope positions in Lecciona are 1, 4, and 13 m^2, while in C4, 951, 4, and 1 m^2, respectively. The conversion of slope and TWI in dynamic variables only worsened their capacity to control the type of soil moisture response in C4. Apart from precipitation/TWI in Lecciona, the dynamic version of local slope and TWI performed better than precipitation itself in all cases in both sites. The culmination of the variability between the two sites was the poor influence of the ASM conditions in C4. The addition of precipitation to ASI slightly improved its performance. One common element between the two sites was the different rankings produced between MDA and MDGI.

The performance of the RF models was further evaluated based on the final rank, calculated as the Euclidean distance between the out-of-bag (OOB) error and the mean absolute prediction error (Eq. (4). For

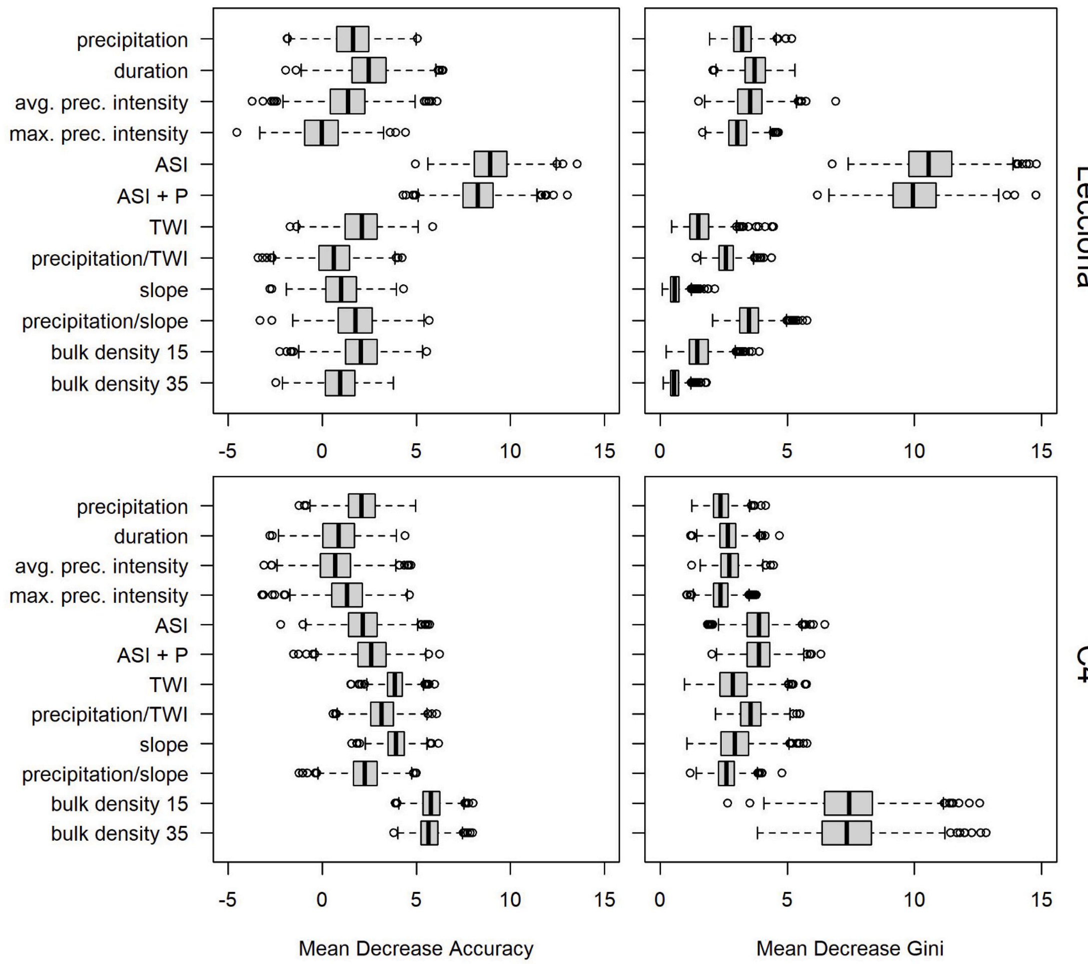

Fig. 8. Box and whisker plots of the mean decrease accuracy (left panels) and mean decrease Gini index (right panels) for each of the twelve potential controlling factors in Lecciona and C4 (see Table 1). The boxes represent the first and third quartiles, the error bars represent the minimum and maximum values, while the data points and the black vertical lines are the outliers and the median, respectively. Precipitation/TWI and Precipitation/slope are the dynamic versions of the static parameters TWI and slope, respectively, as described in Section 2.5. High MDA and MDGI values indicate that a feature is very important for the RF model, and thus for predicting the type of soil moisture response, while low values indicate that the feature has little or no impact on model performance.

Lecciona, the best-performing model for classifying soil moisture response types was achieved using four out of twelve features and a total of 94 trees, resulting in a final rank of 0.37 for non-SEQ responses and 0.11 for SEQ responses. For the C4 hillslope, the optimal configuration was found using two features and 68 trees, achieving final ranks of 0.28 and 0.11 for non-SEQ and SEQ responses, respectively. These values reflect a stronger classification performance for SEQ responses in both study areas, with slightly more difficulty in classifying non-SEQ responses, particularly in Lecciona.

3.2. *Streamflow generation during preferential flow-dominated events*

Normalized hydrographs for the three soil moisture response groups revealed distinct patterns. Although non-SEQ events, i.e., events that generated PF (green line in Fig. 9) did not show the highest streamflow peaks, they presented a first peak relatively early in the hydrograph and mostly a second, large increase sustaining higher streamflow later in the event compared to events that did not generate PF. Events characterized by SEQ responses only (blue line) exhibited, overall, the lowest streamflow with a considerably long recession. Events characterized by a mixed occurrence of SEQ and non-SEQ soil moisture responses (red line) showed the highest peak and displayed a moderate lag between the event onset and peak streamflow. Considering the area under each hydrograph, events associated with PF produced overall 13 % more water volume than mixed events and 31.5 % more water volume than events associated with SEQ responses. The soil moisture responses by hillslope position for precipitation events associated with hydrograph analysis are shown in Table S3 in the Supplementary Material Section.

The standard error of the time to peak and the duration of hydrographs observed in the Lecciona events during the monitoring period ranged from moderate to substantial (Table 3). An exception to this trend was the hydrograph duration for SEQ flows, which exhibited a particularly large standard error. Events characterized by non-SEQ and SEQ soil moisture responses showed shorter times to peak compared to mixed events, while SEQ events exhibited the longest hydrograph durations. Particularly, considering the time to peak/hydrograph duration ratio, there is a clear trend of values (Non-SEQ > Mixed > SEQ) indicating that events with non-SEQ responses had the shortest duration compared to the other events (Table 3).

Although non-statistically significant, the median values of log (Q_{peak}) indicated that events characterized by non-SEQ soil moisture responses resulted in the lowest peak streamflow values, mixed events in intermediate peak streamflows, while the events with SEQ soil moisture response produced the highest peak streamflows (Fig. 10a). The events with SEQ responses presented higher variability in the peak streamflow compared to the non-SEQ events with non-SEQ responses, which had the narrowest IQR range. The events with mixed and SEQ responses maintained their medians' difference (although non-statistically significant)

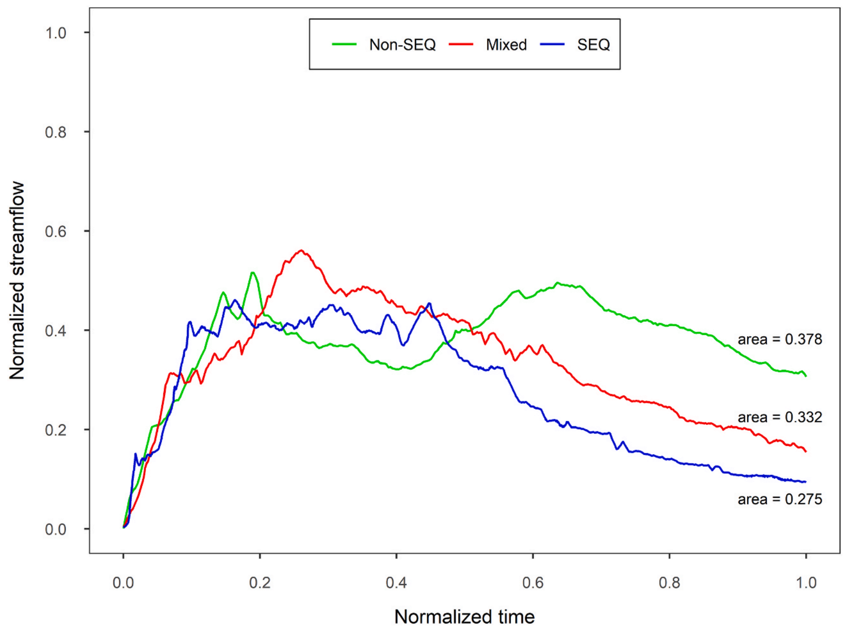

Fig. 9. Average normalized hydrographs for three soil moisture response types in Lecciona, derived from 13 events with non-SEQ soil moisture responses, 20 events with Mixed responses, and 14 events with SEQ responses. The numbers in the legend denote the different numbers of multiple soil moisture responses in the same position within the same event.

Table 3
Average and standard deviation (SD) of the time to hydrograph peak from the start of the event, duration of the hydrograph, and their ratio for the events belonging to the tree groups of soil moisture responses reported in Figs. 8 and 9.

Soil moisture response	Average time to peak ± SE (hr)	Average hydrograph duration ± SD (hr)	Time to peak/ hydrograph duration ratio (–)
Non-SEQ	7.2 ± 2.5	18.5 ± 3.8	0.39
Mixed	8.6 ± 2.2	32.9 ± 4.8	0.26
SEQ	6.8 ± 2.1	48.8 ± 18.9	0.14

also in the logarithmic runoff coefficient, log(RC), with the largest log (RC)s associated with events with SEQ responses. Events with non-SEQ responses presented an overall higher variability of RC compared to the two other types and a higher median RC.

4. Discussion

4.1. Controls on preferential flow

Seasonality in soil moisture response types manifests with PF responses predominantly occurring during wet periods (Figs. 4 and 5), because wet conditions dominate the study period. However, the non-

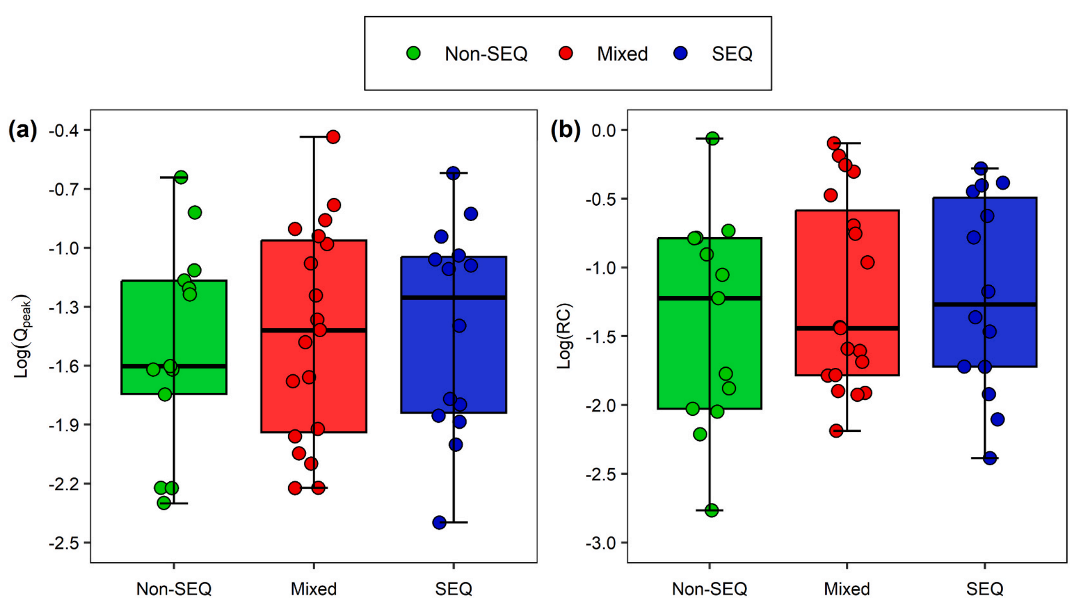

Fig. 10. Box-and-whisker plots with jitter point values of the logarithmic values of a) peak streamflow and b) runoff coefficient by soil moisture response type in Lecciona. The boxes represent the first and third quartiles, the error bars represent the data within 1.5 times the interquartile range (IQR), and the black horizontal line is the median. A Kruskal-Wallis test at the 0.05 significance level indicated no statistically significant difference between the medians of the groups of events in the two panels.

SEQ response relative frequency in wet and dry periods (Table 2) suggest that dry conditions are more favorable to the occurrence of PF. Previous studies have suggested seasonality as a controlling factor of PF with either dry (Demand et al., 2019; Tang et al., 2020; Wessolek et al., 2008) or wet (Buttle and McDonald, 2002; García-Gamero et al., 2021; Nieber and Sidle, 2010) conditions facilitating the phenomenon. The occurrence of PF also depends on factors such as the climatic zone, as well as on the topographic, hydrological and pedological characteristics.

In our study, the riparian position in Lecciona is the only exception to this pattern (Fig. 5). The three hillslope positions in Lecciona have similar soil characteristics and nearly identical canopy cover, as shown by Sentinel-2 LAI values (Section 2.2). However, the riparian zone differs in one key way: it is covered by a thick layer of broadleaf litter from *Fagus sylvatica* trees, which accumulates at the bottom of the slope (Fig. 2). This indicates, first, a rainwater retention by the litter layer, which, due to the higher temperatures in the dry period, evaporates before wetting the shallow layer, and second, a PF path from the footslope to the riparian position. The capacity of litter to intercept infiltration has already been highlighted by Zhu et al. (2020) in a forested hillslope in China, and especially by (Sato et al., 2004), who used a rainfall simulator and demonstrated the enhanced interception storage capacity of broad-leaf litter, which even increased with precipitation intensity. More importantly, they observed a lateral movement of penetrating water in the broad-leaf litter, contrasting it with the vertical movement observed in needle-leaf litter (e.g., coniferous species).

In C4, all probes at 15 cm depth remained unresponsive following extended dry periods, whereas the 35 cm layer showed a quick response to precipitation after drought conditions. This suggests a high occurrence of PF under such conditions, which is confirmed by the multiple non-SEQ responses that often occur right after large gaps in the hyetograph (Fig. 4). Many of these non-SEQ responses are marked by a response only at 35 cm without a succeeding response at 15 cm, revealing a possible routing of rainfall water directly at the deeper soil entirely bypassing the shallow layer. Most of the events that lead to SEQ responses at the top position yielded non-SEQ responses at the middle, which strongly indicates lateral flow from the top to the middle position. This agrees with the previous results from a Spanish Mediterranean catchment where soil moisture observations along a north-facing and a south-facing hillslope revealed similar disconnections between positions of the same hillslope suggesting lateral redistribution of soil moisture from top to bottom (García-Gamero et al., 2021).

Despite the subtle propensity of low precipitation characteristics (depth, duration, and maximum intensity) to trigger PF in both Lecciona and C4 (Figs. 6a–c and Figs. 7a–c), the role of precipitation (including all its properties) as a control of PF remains ambiguous at both sites. The influence of precipitation properties as a proxy for PF appears to be not only site-specific but position-specific, especially in C4 (Figs. 7b and c). This complex behavior is clearly reflected in literature, where numerous studies emphasize the role of precipitation properties as key factors driving soil moisture dynamics (e.g., Demand et al., 2019; Graham and Lin, 2011; Tymchak and Torres, 2007; Wiekenkamp et al., 2016; Yan and Zhao, 2016). However, a similarly extensive body of research presents opposing conclusions, suggesting that precipitation properties are less influential in shaping these dynamics (e.g., Dusek and Vogel, 2016; Liu and Lin, 2015; Nanda and Safeeq, 2023; Singh et al., 2021; Williams et al., 2023). Together, these findings underscore the unpredictable and erratic nature of PF dynamics. Dusek and Vogel (2016) used both synthetic and natural rainfall data to analyze the effect of precipitation characteristics on hillslope runoff in a small, forested headwater catchment in the Czech Republic but did not end up with a consistent amount of precipitation that initiated PF. Liu and Lin (2015) analyzed 412 events at 35 sites in the forested hilly catchment of Shale Hills in central Pennsylvania (USA) and found precipitation properties to be site specific in inducing PF. The ambiguity observed in the studies by Dusek and Vogel (2016) and Liu and Lin (2015) is similarly evident in our case.

In Lecciona higher ASI values (Fig. 6d) showed that events with high ASM were more likely to trigger PF. When precipitation depth was added (Fig. 6e), this trend remained, though the data showed less variability. The situation was different in C4, where ASM appeared to be position sensitive with higher ASI values favoring PF only in the middle hillslope position. This is in agreement with the findings of Tang et al. (2020), who also found antecedent wetness to be site- and position-sensitive. The RF application successfully captured the strong relationship between ASM values and PF occurrence in Lecciona (Fig. 8). This is further supported by the variable importance metrics from the RF model, where ASM exhibited the highest values among all predictors: MDA 9.0 for ASI and 8.3 for ASI + P, while MDGI 10.6 for ASI and 10.0 for ASI + P, confirming ASM's dominant role in driving PF in Lecciona.

According to Fig. 7d, ASM conditions were not deemed a strong driver of PF occurrence by the RF simulation at C4, which instead highlighted soil dry bulk density as a key determinant of PF. The corresponding MDA values for C4 were 5.8 for dry bulk density at 15 cm and 5.7 at 35 cm, while the MDGI values were 7.4 dry bulk density at 15 cm and 7.3 at 35 cm (Fig. 8). The soil dry bulk density measurements showed a more compacted, less porous soil in C4 compared to Lecciona, where overall smaller bulk density values were measured. This was somewhat surprising, especially given that 160 PF responses were triggered in C4 compared to 139 in Lecciona in almost half the time and half the precipitation events. These numbers also account for multiple PF responses (up to six) occurring within certain individual precipitation events. Though counterintuitive, high infiltration rates and PF in compacted soils are not so uncommon. However, Wuest (2009) in his dye tracer experiments found that untilled soils with higher bulk density had greater infiltration rates than tilled soils with lower bulk density. Greater bulk density is often associated with greater hydraulic conductivity, which is attributed to fewer but better connected pores (Strudley et al., 2008). Moreover, (Heijs et al., 1996) found finger flow formations, associated with PF, in denser parts of water-repellent sandy soils, suggesting that the menisci of concentrated flow through those fingers pulled soil particles together, leading to higher bulk densities. This suggests that macropores could be responsible for increasing soil compaction, and their presence could be associated with high bulk densities and vice versa. The natural tendency of the denser soil profile in C4 to induce a significantly greater number of PF responses compared to the more porous soil in Lecciona may indicate the presence of macropore structures or hydrophobic parts in the C4 soil profile, possibilities that need to be explored in future studies.

The RF model simulated reality remarkably well, with the results (Fig. 8) aligning closely with the field observations (Figs. 6 and 7). For example, in Lecciona, the RF simulation ranked duration as a more significant control than precipitation depth, which in turn was ranked as more significant than maximum precipitation intensity. This ranking is consistent with the clustering of points at the midslope position that clearly highlights the differences between SEQ and non-SEQ (Figs. 6a–c). Duration had the strongest distinction between these two responses, followed by precipitation depth, and lastly, maximum precipitation intensity. Same reasonings and results apply for C4, where precipitation depth was a stronger control than the other precipitation properties as it was the only one with a consistent trend in all three hillslope positions. The efficiency of the RF model is further demonstrated by the improvement in ASI + P for C4, where adding precipitation improves predictions, whereas for Lecciona adding precipitation leads to a deterioration of the relation with ASI + P. Out of the twelve features examined as potential controls of PF, the best results of the RF model for predicting the type of the soil moisture response were achieved for four features in Lecciona and for two features in C4 (Section S1.1 and Figs. S1 and S2). In one of the rare applications of RF to PF studies, Koestel and Jorda (2014) predicted the soil susceptibility to PF and identified key drivers such as clay content, the ratio between clay and organic carbon, and the lateral observation scale, whereas Zhang et al. (2024) found that clay and sand contents, drainage capacity, and bulk density at different depths were the most important predictors of

PF.

4.2. Effect of preferential flow on streamflow response

The three distinct average normalized hydrographs (Fig. 9) for each soil moisture response group −SEQ, non-SEQ, and mixed events-shed new light on the complex effect of PF on streamflow response. The rapid streamflow increase of PF events (green line in Fig. 9) early in the hydrograph highlights that PF is responsible for fast and increased streamflow responses also in forested catchments, as observed in other environments (Stoof et al., 1969; Zehe et al., 2007; Zehe and Flühler, 2001). Streamflow during events with only SEQ responses (blue line in Fig. 9) was moderate both in terms of response timing and magnitude. Similar findings were presented by Swarowsky et al. (2012) in their study of subsurface flow/streamflow dynamics in a semi-arid Mediterranean headwater catchment in northern California, where low streamflow conditions were always associated with soil matrix flow. Our findings were in line with the generally accepted understanding that PF bypasses most of the soil matrix contributing rapidly to interflow and baseflow, while matrix flow involves slower percolation through small soil pores, resulting in a delayed and reduced contribution to streamflow. However, our study expands this knowledge by showing new evidence that PF is able to sustain higher streamflow later in the event. The high streamflow values observed later in the hydrograph for events that generated PF suggest the development of hillslope-stream subsurface hydrological connectivity that was able to deliver substantial amount of water to the stream and sustain streamflow. Root- and faunal-induced soil macroporosity is often closely associated with preferential flow, and macropore flow can substantially contribute to runoff generation, especially in forested hillslopes and catchments (Weiler, 2017). Therefore, macropores in our study hillslopes might become connected during wet conditions and can stay active for long times, thereby sustaining the supply to the stream. This observation is supported by previous studies that showed that the expansion and extension of macropore networks during large storm events significantly contribute to stormflow of a small forested catchment in Japan (Noguchi et al., 2016), and that the formation of a macropore system combined with preferential pipe flow pathways, formed by the coarse root system of the mature deciduous forest stand, produced a fast runoff reaction in a catchment with mixed land use in Germany (Hümann et al., 2011). Another, not necessarily alternative, explanation lies in the generation of delayed drainage from deeper layers accessed by PF through macropores and soil fissures that feeds the stream during the hydrograph recession (Sidle et al., 2000). The majority of the events were mixed events, i.e., characterized by a mixed occurrence of SEQ and non-SEQ soil moisture responses (red line in Fig. 9). The moderate time lag between the event onset and peak streamflow as well as the long recession suggest a gradual built-up and then disruption of hydrological connectivity. This is reasonable as during precipitation events matrix flow and PF often occur simultaneously and factors like ASM, as well as soil and precipitation characteristics will determine which process is dominant (Lozano-Parra et al., 2016). As the majority of studies focused on matrix flow and/or PF individually, the effect of mixed events on streamflow we showed here is a novel result.

4.3. Limitations and future research

While this study provides new insights into the role of PF in Mediterranean forested catchments, some limitations should be acknowledged. First, the spatial scale of the study is limited to two hillslopes and one catchment. Though PF mechanisms are inherently complex and difficult to generalize (e.g., see literature contradictions regarding precipitation properties in Section 4.1), the spatial limitation of this study remains significant. Second, the soil moisture response classification approach, based on time differences between probe depths, might overlook more subtle preferential flow pathways or interactions with other subsurface processes, such as perched water table dynamics or root water uptake. Future research should integrate complementary tools such as dye tracing or geophysical methods such as ground-penetrating radar to map these flow paths with greater resolution. Additionally, while RF models are generally effective in identifying key predictors, they do not explain the underlying physical processes and may overlook interactions between variables. Incorporating physical modeling or mechanistic process-based simulations in future studies could help validate and expand on the empirical relationships found here.

5. Conclusions

This study investigated the drivers and dynamics of preferential flow (PF) in a Mediterranean forested catchment, focusing on the effects of precipitation characteristics, antecedent soil moisture, soil properties, and topography, as well as on the influence of PF on streamflow. Through extensive field measurements, soil moisture monitoring, and the application of a random forest model, we gained new insights into the complex controls of PF initiation in forested catchments, especially missing in the Mediterranean region, characterized by an alternation of wet and dry periods.

PF-generating precipitation events resulted in the highest connectivity and sustained streamflow, sequential events exhibited minimal connectivity and streamflow, and mixed-response events produced moderate connectivity and the highest overall streamflow with the longest recession.

The RF model was a key methodological innovation, allowing for the identification of site-specific controls on PF. In Lecciona, antecedent soil moisture was identified as the primary driver of PF, emphasizing the importance of pre-storm conditions. In C4, dry bulk density emerged as the dominant control, highlighting the role of soil compaction. These findings underscore the variability of PF controls across different sites and conditions. Our findings are of particular significance, especially because they contribute to gaining new understanding of hydrological dynamics of Mediterranean forested mountain catchments. These systems are intrinsically complex due to the superimposition of the seasonality of the meteorological inputs that creates contrasting moisture conditions reflected in marked differences of streamflow response, and the role of harsh topography and dense vegetation cover. Our results shed new light on the controls on preferential flow triggering and its role in runoff generation, contributing to highlight the importance of these processes in seasonally dry and wet hydrological systems, as the Mediterranean catchments.

Future research should investigate the role of macropore structures and soil hydrophobicity in influencing preferential flow dynamics, as well as expand the application of machine learning techniques to better understand PF controls and its the effect of PF on catchment hydrological response in Mediterranean settings.

Funding and acknowledgements

This study was supported by the following research projects: “WATer mixing in the critical ZONe: observations and predictions under environmental changes – WATZON” (call PRIN 2017, code: 2017SL7ABC), funded by the Italian Ministry of University and Research (MUR); “Unravelling interactions between WATER and carbon cycles during drought and their impact on water resources and forest and grassland ecosySTEMs in the Mediterranean climate – WATERSTEM” (call PRIN 2020, code: 20202WF53Z), funded by the Italian Ministry of University and Research (MUR); “Carbon and water cycles interactions during drought and their impact on WAter and ForEst Resources in the Mediterranean region −WAFER” (code: B95F21002170001) funded by the Italian National research Council (Consiglio Nazionale delle Ricerche – CNR); “Hydrological controls on carbonate-mediated CO2 consumptions – HYDRO4C (call PRIN 2022, code: 2022PFNNRS) funded by the European Union, Next Generation EU; and “Space It Up!” (call ASI n. 687/

2022 of 26 July 2022, contract ASI N. 2024–5-E.0, master code: I53D24000060005, WP 7.6), funded by the Italian Space Agency (ASI) and the Italian Ministry of University and Research (MUR). The authors thank the local Forest Service (Unione Comuni Valdarno e Valdisieve) for their logistical support in managing the Re della Pietra experimental catchment. K.K. was supported by the WATERSTEM project. M.M.G. acknowledges his support by the FONDECYT Postdoctoral Grant 3220318 funded by the Chilean Agency of Research and Development (ANID).

We would further like to thank Antonello Maruotti, Professor at the Department of Law, Economics, Politics and Modern Languages, Libera Università Maria Ss Assunta, for his valuable suggestions in the Random Forest analysis. Our thanks extend to Lutz Klein for his contribution to the soil sampling campaign in the Re della Pietra catchment.

CRediT authorship contribution statement

K. Kaffas: Writing – review & editing, Writing – original draft, Visualization, Validation, Software, Resources, Project administration, Methodology, Investigation, Formal analysis, Data curation, Conceptualization. **I. Murgia:** Writing – review & editing, Writing – original draft, Validation, Resources, Methodology, Investigation, Formal analysis, Data curation, Conceptualization. **A. Menapace:** Writing – review & editing, Writing – original draft, Visualization, Validation, Software, Methodology, Investigation, Formal analysis, Data curation, Conceptualization. **M. Macchioli Grande:** Writing – review & editing, Writing – original draft, Investigation, Data curation, Formal analysis. **M. Verdone:** Writing – review & editing, Methodology, Investigation, Formal analysis, Data curation. **A. Dani:** Writing – review & editing, Methodology, Investigation. **F.S. Manca di Villahermosa:** Writing – review & editing, Methodology, Investigation, Data curation. **F. Preti:** Writing – review & editing, Methodology, Investigation. **C. Segura:** Writing – review & editing, Methodology, Investigation, Conceptualization. **C. Massari:** Writing – review & editing, Methodology, Investigation, Funding acquisition, Conceptualization. **J. Klaus:** Writing – review & editing, Methodology, Investigation, Conceptualization. **M. Borga:** Writing – review & editing, Methodology, Investigation. **D. Penna:** Writing – review & editing, Writing – original draft, Visualization, Validation, Supervision, Software, Resources, Project administration, Methodology, Investigation, Funding acquisition, Formal analysis, Data curation, Conceptualization.

Declaration of competing interest

The authors declare that they have no known competing financial interests or personal relationships that could have appeared to influence the work reported in this paper.

Appendix A. Supplementary material

Supplementary data to this article can be found online at https://doi.org/10.1016/j.jhydrol.2025.133469.

Data availability

Data will be made available on request.

References

Ali, G., Tetzlaff, D., Mcdonnell, J.J., Soulsby, C., Carey, S., Laudon, H., Mcguire, K., Buttle, J., Seibert, J., Shanley, J., 2015. Comparison of threshold hydrologic response across northern catchments. Hydrol. Process. 29, 3575–3591. https://doi.org/10.1002/hyp.10527.

Allaire, S.E., Roulier, S., Cessna, A.J., 2009. Quantifying preferential flow in soils: a review of different techniques. J. Hydrol. 378, 179–204. https://doi.org/10.1016/j.jhydrol.2009.08.013.

Amendola, U., Perri, F., Critelli, S., Monaco, P., Cirilli, S., Trecci, T., Rettori, R., 2016. Composition and provenance of the Macigno formation (Late Oligocene-Early Miocene) in the Trasimeno Lake area (Northern Apennines). Mar. Pet. Geol. 69, 146–167. https://doi.org/10.1016/j.marpetgeo.2015.10.019.

Assouline, S., Ben-Hur, M., 2006. Effects of rainfall intensity and slope gradient on the dynamics of interrill erosion during soil surface sealing. Catena 66, 211–220. https://doi.org/10.1016/j.catena.2006.02.005.

Avanzi, F., Johnson, R.C., Oroza, C.A., Hirashima, H., Maurer, T., Yamaguchi, S., 2019. Insights into preferential flow snowpack runoff using random forest. Water Resour. Res. 55, 10727–10746. https://doi.org/10.1029/2019WR024828.

Bai, H., Liu, L., Han, Q., Zhao, Y., Zhao, Y., 2023. A novel UNet segmentation method based on deep learning for preferential flow in soil. Soil Tillage Res. 233, 105792. https://doi.org/10.1016/j.still.2023.105792.

Bauters, T.W.J., Steenhuis, T.S., Parlange, J., DiCarlo, D.A., 1998. Preferential flow in water-repellent sands. Soil Sci. Soc. Am. J. 62, 1185–1190. https://doi.org/10.2136/sssaj1998.03615995006200050005x.

Beven, K., Germann, P., 2013. Macropores and water flow in soils revisited. Water Resour. Res. 49, 3071–3092. https://doi.org/10.1002/wrcr.20156.

Beven, K., Germann, P., 1982. Beven and Germann, 1982.pdf. Water Resour. Res. 18, 1311–1325. https://doi.org/10.1029/WR018i005p01311.

Beven, K.J., Kirkby, M.J., 1979. A physically based, variable contributing area model of basin hydrology. Hydrol. Sci. Bull. 24, 43–69. https://doi.org/10.1080/02626667909491834.

Blume, T., van Meerveld, H.J., 2015. From hillslope to stream: methods to investigate subsurface connectivity. Wiley Interdiscip. Rev. Water 2, 177–198. https://doi.org/10.1002/WAT2.1071.

Breiman, L., 2001. RFRSF: employee turnover prediction based on random forests and survival analysis. Mach. Learn. 45, 5–32.

Buttle, J.M., McDonald, D.J., 2002. Coupled vertical and lateral preferential flow on a forested slope. Water Resour. Res. 38, 18–1-18–16. https://doi.org/10.1029/2001wr000773.

Cain, M.R., Woo, D.K., Kumar, P., Keefer, L., Ward, A.S., 2022. Antecedent conditions control thresholds of tile-runoff generation and nitrogen export in intensively managed landscapes. Water Resour. Res. 58, 1–18. https://doi.org/10.1029/2021WR030507.

Carranza, C., Nolet, C., Pezij, M., van der Ploeg, M., 2021. Root zone soil moisture estimation with Random Forest. J. Hydrol. 593, 125840. https://doi.org/10.1016/j.jhydrol.2020.125840.

Clothier, B.E., Green, S.R., Deurer, M., 2008. Preferential flow and transport in soil: progress and prognosis. Eur. J. Soil Sci. 59, 2–13. https://doi.org/10.1111/j.1365-2389.2007.00991.x.

Dekker, L.W., Ritsema, C.J., 1994. How water moves in a water repellent sandy soil: 1. Potential and actual water repellency. Water Resour. Res. 30, 2507–2517. https://doi.org/10.1029/94WR00749.

Demand, D., Blume, T., Weiler, M., 2019. Spatio-temporal relevance and controls of preferential flow at the landscape scale. Hydrol. Earth Syst. Sci. 23, 4869–4889. https://doi.org/10.5194/hess-23-4869-2019.

Desai, S., Ouarda, T.B.M.J., 2021. Regional hydrological frequency analysis at ungauged sites with random forest regression. J. Hydrol. 594, 125861. https://doi.org/10.1016/j.jhydrol.2020.125861.

Detty, J.M., McGuire, K.J., 2010. Threshold changes in storm runoff generation at a till-mantled headwater catchment. Water Resour. Res. 46, 1–15. https://doi.org/10.1029/2009WR008102.

Dusek, J., Vogel, T., 2016. Hillslope-storage and rainfall-amount thresholds as controls of preferential stormflow. J. Hydrol. 534, 590–605. https://doi.org/10.1016/j.jhydrol.2016.01.047.

Dymond, S.F., Wagenbrenner, J.W., Keppeler, E.T., Bladon, K.D., 2021. Dynamic hillslope soil moisture in a Mediterranean montane watershed. Water Resour. Res. 57, 1–22. https://doi.org/10.1029/2020WR029170.

Fabiani, G., Klaus, J., Penna, D., 2024. The influence of hillslope topography on beech water use: a comparative study in two different climates. Hydrol. Earth Syst. Sci. 28, 2683–2703. https://doi.org/10.5194/hess-28-2683-2024.

Flury, M., Flühler, H., Jury, W.A., Leuenberger, J., 1994. Susceptibility of soils to preferential flow of water: a field study. Water Resour. Res. 30, 1945–1954. https://doi.org/10.1029/94WR00871.

Franklin, S.M., Kravchenko, A.N., Vargas, R., Vasilas, B., Fuhrmann, J.J., Jin, Y., 2021. The unexplored role of preferential flow in soil carbon dynamics. Soil Biol. Biochem. 161, 108398. https://doi.org/10.1016/j.soilbio.2021.108398.

Gagkas, Z., Lilly, A., 2019. Downscaling soil hydrological mapping used to predict catchment hydrological response with random forests. Geoderma 341, 216–235. https://doi.org/10.1016/j.geoderma.2019.01.048.

García-Gamero, V., Peña, A., Laguna, A.M., Giráldez, J.V., Vanwalleghem, T., 2021. Factors controlling the asymmetry of soil moisture and vegetation dynamics in a hilly Mediterranean catchment. J. Hydrol. 598. https://doi.org/10.1016/j.jhydrol.2021.126207.

Gazis, C., Feng, X., 2004. A stable isotope study of soil water: Evidence for mixing and preferential flow paths. Geoderma 119, 97–111. https://doi.org/10.1016/S0016-7061(03)00243-X.

Gong, H., Pan, Y., Xu, Y., 2012. Variation spatio-temporelle de la recharge des eaux souterraines en réponse à la variabilité des sols, des précipitations et de l'occupation des sols, Bassin de Yanqing, Beijing. Chine. Hydrogeol. J. 20, 1331–1340. https://doi.org/10.1007/s10040-012-0883-x.

Graham, C.B., Lin, H.S., 2011. Controls and frequency of preferential flow occurrence: a 175-event analysis. Vadose Zo. J. 10, 816–831. https://doi.org/10.2136/vzj2010.0119.

Grant, K.N., Macrae, M.L., Ali, G.A., 2019. Differences in preferential flow with antecedent moisture conditions and soil texture: implications for subsurface P transport. Hydrol. Process. 33, 2068–2079. https://doi.org/10.1002/hyp.13454.

Greve, A.K., Andersen, M.S., Acworth, R.I., 2012. Monitoring the transition from preferential to matrix flow in cracking clay soil through changes in electrical anisotropy. Geoderma 179–180, 46–52. https://doi.org/10.1016/j.geoderma.2012.02.003.

Guo, L., Lin, H., 2018. Addressing Two Bottlenecks to Advance the Understanding of Preferential Flow in Soils. In: Advances in Agronomy, 1st ed,. Elsevier Inc. https://doi.org/10.1016/bs.agron.2017.10.002

Guo, L., Lin, H., Fan, B., Nyquist, J., Toran, L., Mount, G.J., 2019. Preferential flow through shallow fractured bedrock and a 3D fill-and-spill model of hillslope subsurface hydrology. J. Hydrol. 576, 430–442. https://doi.org/10.1016/j.jhydrol.2019.06.070.

Haga, H., Matsumoto, Y., Matsutani, J., Fujita, M., Nishida, K., Sakamoto, Y., 2005. Flow paths, rainfall properties, and antecedent soil moisture controlling lags to peak discharge in a granitic unchanneled catchment. Water Resour. Res. 41, 1–14. https://doi.org/10.1029/2005WR004236.

Hangen, E., Gerke, H.H., Schaaf, W., Hüttl, R.F., 2005. Assessment of preferential flow processes in a forest-reclaimed lignitic mine soil by multicell sampling of drainage water and three tracers. J. Hydrol. 303, 16–37. https://doi.org/10.1016/j.jhydrol.2004.07.009.

Hardie, M.A., Cotching, W.E., Doyle, R.B., Holz, G., Lisson, S., Mattern, K., 2011. Effect of antecedent soil moisture on preferential flow in a texture-contrast soil. J. Hydrol. 398, 191–201. https://doi.org/10.1016/j.jhydrol.2010.12.008.

Heijs, A.W.J., Ritsema, C.J., Dekker, L.W., 1996. Three-dimensional visualization of preferential flow patterns in two soils. Geoderma 70, 101–116. https://doi.org/10.1016/0016-7061(95)00076-3.

Heppell, C.M., Worrall, F., Burt, T.P., Williams, R.J., 2002. A classification of drainage and macropore flow in an agricultural catchment. Hydrol. Process. 16, 27–46. https://doi.org/10.1002/hyp.282.

Hopkins, I., Gall, H., Lin, H., 2016. Natural and anthropogenic controls on the frequency of preferential flow occurrence in a wastewater spray irrigation field. Agric Water Manag 178, 248–257. https://doi.org/10.1016/j.agwat.2016.09.011.

Hosking, J.G., Stow, C.D., Bradley, S.G., 1985. Corrections for horizontal winds and wind shear in raindrop size spectrometers. J. Atmos. Ocean. Technol. 2, 181–189. https://doi.org/10.1175/1520-0426(1985)002<0181:CFHWAW>2.0.CO;2.

Hümann, M., Schüler, G., Müller, C., Schneider, R., Johst, M., Caspari, T., 2011. Identification of runoff processes - the impact of different forest types and soil properties on runoff formation and floods. J. Hydrol. 409, 637–649. https://doi.org/10.1016/j.jhydrol.2011.08.067.

Jarvis, N., Koestel, J., Larsbo, M., 2016. Understanding preferential flow in the vadose zone: recent advances and future prospects. Vadose Zo. J. 15, 1–11. https://doi.org/10.2136/vzj2016.09.0075.

Jarvis, N.J., 2007. A review of non-equilibrium water flow and solute transport in soil macropores: principles, controlling factors and consequences for water quality. Eur. J. Soil Sci. 58, 523–546. https://doi.org/10.1111/j.1365-2389.2007.00915.x.

Kang, W., Tian, J., Reemt Bogena, H., Lai, Y., Xue, D., He, C., 2023. Soil moisture observations and machine learning reveal preferential flow mechanisms in the Qilian Mountains. Geoderma 438. https://doi.org/10.1016/j.geoderma.2023.116626.

Kocian, L., Mohanty, B.P., 2024. Characterizing large-scale preferential flow across Continental United States. Vadose Zo. J. 23, 1–19. https://doi.org/10.1002/vzj2.20316.

Koestel, J., Jorda, H., 2014. What determines the strength of preferential transport in undisturbed soil under steady-state flow? Geoderma 217–218, 144–160. https://doi.org/10.1016/j.geoderma.2013.11.009.

Köhne, J.M., Mohanty, B.P., Šimůnek, J., 2006. Inverse dual-permeability modeling of preferential water flow in a soil column and implications for field-scale solute transport. Vadose Zo. J. 5, 59–76. https://doi.org/10.2136/vzj2005.0008.

Kulasekera, P.B., Parkin, G.W., von Bertoldi, P., 2011. Using soil water content sensors to characterize tillage effects on preferential flow. Vadose Zo. J. 10, 683–696. https://doi.org/10.2136/vzj2010.0063.

Lam, W.V., Macrae, M.L., English, M.C., O'Halloran, I.P., Plach, J.M., Wang, Y., 2016. Seasonal and event-based drivers of runoff and phosphorus export through agricultural tile drains under sandy loam soil in a cool temperate region. Hydrol. Process. 30, 2644–2656. https://doi.org/10.1002/hyp.10871.

Li, L., Wu, D., Wang, T., Wang, Y., 2022. Effect of topography on spatiotemporal patterns of soil moisture in a mountainous region of Northwest China. Geoderma Reg. 28, e00456. https://doi.org/10.1016/j.geodrs.2021.e00456.

Lin, H., Zhou, X., 2008. Evidence of subsurface preferential flow using soil hydrologic monitoring in the Shale Hills catchment. Eur. J. Soil Sci. 59, 34–49. https://doi.org/10.1111/j.1365-2389.2007.00988.x.

Liu, H., Lin, H., 2015. Frequency and control of subsurface preferential flow: from Pedon to catchment scales. Soil Sci. Soc. Am. J. 79, 362–377. https://doi.org/10.2136/sssaj2014.08.0330.

Lozano-Parra, J., van Schaik, N.L.M.B., Schnabel, S., Gómez-Gutiérrez, Á., 2016. Soil moisture dynamics at high temporal resolution in a semiarid Mediterranean watershed with scattered tree cover. Hydrol. Process. 30, 1155–1170. https://doi.org/10.1002/hyp.10694.

Macchioli Grande, M., Kaffas, K., Verdone, M., Borga, M., Cocozza, C., Dani, A., Errico, A., Fabiani, G., Gourdol, L., Klaus, J., Manca di Villahermosa, F.S., Massari, C., Murgia, I., Pfister, L., Preti, F., Segura, C., Tailliez, C., Trucchi, P., Zuecco, G., Penna, D., 2024. Seasonal meteorological forcing controls runoff generation at multiple scales in a Mediterranean forested mountain catchment. J. Hydrol. 639, 131642. https://doi.org/10.1016/j.jhydrol.2024.131642.

Marsalek, J., 1981. Calibration of the tipping-bucket raingage. J. Hydrol. 53, 343–354. https://doi.org/10.1016/0022-1694(81)90010-X.

Mooney, S.J., Morris, C., 2008. A morphological approach to understanding preferential flow using image analysis with dye tracers and X-ray computed tomography. Catena 73, 204–211. https://doi.org/10.1016/j.catena.2007.09.003.

Nanda, A., Safeeq, M., 2023. Threshold controlling runoff generation mechanisms in Mediterranean headwater catchments. J. Hydrol. 620, 129532. https://doi.org/10.1016/j.jhydrol.2023.129532.

Nanda, A., Sen, S., McNamara, J.P., 2019. How spatiotemporal variation of soil moisture can explain hydrological connectivity of infiltration-excess dominated hillslope: observations from lesser Himalayan landscape. J. Hydrol. 579, 124146. https://doi.org/10.1016/j.jhydrol.2019.124146.

Nguyen, Q.H., Ly, H.B., Ho, L.S., Al-Ansari, N., Van Le, H., Tran, V.Q., Prakash, I., Pham, B.T., 2021. Influence of data splitting on performance of machine learning models in prediction of shear strength of soil. Math. Probl. Eng. 2021. https://doi.org/10.1155/2021/4832864.

Nieber, J.L., Sidle, R.C., 2010. How do disconnected macropores in sloping soils facilitate preferential flow? Hydrol. Process. 24, 1582–1594. https://doi.org/10.1002/hyp.7633.

Noguchi, S., Kaneko, T., Iida, S., Murakami, W., Shimizu, T., 2016. Effects of vegetation and soil on evapotranspiration, flow regime, and basin storage in three nearby catchments in northeast Japan. Hydrol. Earth Syst. Sci. Discuss. 1–22. https://doi.org/10.5194/hess-2016-616.

Noguchi, S., Tsuboyama, Y., Sidle, R.C., Hosoda, I., 1999. Morphological characteristics of macropores and the distribution of preferential flow pathways in a forested slope segment. Soil Sci. Soc. Am. J. 63, 1413–1423. https://doi.org/10.2136/sssaj1999.6351413x.

Papacharalampous, G., Tyralis, H., 2022. A review of machine learning concepts and methods for addressing challenges in probabilistic hydrological post-processing and forecasting. Front. Water 4. https://doi.org/10.3389/frwa.2022.961954.

Penna, D., van Meerveld, H.J., Oliviero, O., Zuecco, G., Assendelft, R.S., Dalla Fontana, G., Borga, M., 2015. Seasonal changes in runoff generation in a small forested mountain catchment. Hydrol. Process. 29, 2027–2042. https://doi.org/10.1002/hyp.10347.

Radolinski, J., Pangle, L., Klaus, J., Stewart, R.D., 2021. Testing the 'two water worlds' hypothesis under variable preferential flow conditions. Hydrol. Process. 35, 1–14. https://doi.org/10.1002/hyp.14252.

Rinehart, R.E., 1983. Out-of-level instruments: errors in hydrometeor spectra and precipitation measurements. J. Clim. Appl. Meteorol. 22, 1404–1410. https://doi.org/10.1175/1520-0450(1983)022<1404:OOLIEI>2.0.CO;2.

Sato, Y., Kumagai, T., Kume, A., Otsuki, K., Ogawa, S., 2004. Experimental analysis of moisture dynamics of litter layers - the effects of rainfall conditions and leaf shapes. Hydrol. Process. 18, 3007–3018. https://doi.org/10.1002/hyp.5746.

Schoppa, L., Disse, M., Bachmair, S., 2020. Evaluating the performance of random forest for large-scale flood discharge simulation. J. Hydrol. 590, 125531. https://doi.org/10.1016/j.jhydrol.2020.125531.

Sidle, R.C., Kitahara, H., Terajima, T., Nakai, Y., 1995. Experimental studies on the effects of pipeflow on throughflow partitioning. J. Hydrol. 165, 207–219. https://doi.org/10.1016/0022-1694(94)02563-Q.

Sidle, R.C., Noguchi, S., Tsuboyama, Y., Laursen, K., 2001. A conceptual model of preferential flow systems in forested hillslopes: evidence of self-organization. Hydrol. Process. 15, 1675–1692. https://doi.org/10.1002/hyp.233.

Sidle, R.C., Tsuboyama, Y., Noguchi, S., Hosoda, I., Fujieda, M., Shimizu, T., 2000. Stormflow generation in steep forested headwaters: a linked hydrogeomorphic paradigm. Hydrol. Process. 14, 369–385. https://doi.org/10.1002/(SICI)1099-1085(20000228)14:3<369::AID-HYP943>3.0.CO;2-P.

Singh, N.K., Emanuel, R.E., McGlynn, B.L., Miniat, C.F., 2021. Soil moisture responses to rainfall: implications for runoff generation. Water Resour. Res. 57, 1–17. https://doi.org/10.1029/2020WR028827.

Solomatine, D.P., Ostfeld, A., 2008. Data-driven modelling: some past experiences and new approaches. J. Hydroinformatics 10, 3–22. https://doi.org/10.2166/hydro.2008.015.

Song, S., Wang, W., 2019. Impacts of antecedent soil moisture on the rainfall- runoff transformation process based on high- resolution observations in soil tank experiments. Water (Switzerland) 11, 15–20. https://doi.org/10.3390/w11020296.

Stoof, C.R., Slingerland, E.C., Mol, W., van den Berg, J., Vermeulen, P.J., Ferreira, A.J.D., Ritsema, C.J., Parlange, J.-Y., Steenhuis, T.S., 1969. Water resources research. Water Resour. Res. 50, 1840–1845. https://doi.org/10.1002/2013WR014397.

Strudley, M.W., Green, T.R., Ascough, J.C., 2008. Tillage effects on soil hydraulic properties in space and time: State of the science. Soil Tillage Res. 99, 4–48. https://doi.org/10.1016/j.still.2008.01.007.

Swarowsky, A., Dahlgren, R.A., O'Geen, A.T., 2012. Linking subsurface lateral flowpath activity with streamflow characteristics in a semiarid headwater catchment. Soil Sci. Soc. Am. J. 76, 532–547. https://doi.org/10.2136/sssaj2011.0061.

Sypka, P., 2019. Dynamic real-time volumetric correction for tipping-bucket rain gauges. Agric. For. Meteorol. 271, 158–167. https://doi.org/10.1016/j.agrformet.2019.02.044.

Tang, Q., Duncan, J.M., Guo, L., Lin, H., Xiao, D., Eissenstat, D.M., 2020. On the controls of preferential flow in soils of different hillslope position and lithological origin. Hydrol. Process. 34, 4295–4306. https://doi.org/10.1002/hyp.13883.

Thornthwaite, C.W., 1948. An approach toward a rational classification of climate C. W. Thornthwaite. Geogr. Rev. 38, 55–94.

Tromp-Van Meerveld, H.J., McDonnell, J.J., 2006. Threshold relations in subsurface stormflow: 1. A 147-storm analysis of the Panola hillslope. Water Resour. Res. 42, 1–11. https://doi.org/10.1029/2004WR003778.

Tsuboyama, Y., Sidle, R.C., Noguchi, S., Hosoda, I., 1994. Flow and solute transport through the soil matrix and macropores of a hillslope segment. Water Resour. Res. 30, 879–890. https://doi.org/10.1029/93WR03245.

Tymchak, M.P., Torres, R., 2007. Effects of variable rainfall intensity on the unsaturated zone response of a forested sandy hillslope. Water Resour. Res. 43, 1–13. https://doi.org/10.1029/2005WR004584.

Uchida, T., Kosugi, K.N.I., Mizuyama, T., 2001. Effects of pipeflow on hydrological process and its relation to landslide: a review of pipeflow studies in forested headwater catchments. Hydrol. Process. 15, 2151–2174. https://doi.org/10.1002/hyp.281.

Uchida, T., Tromp-Van Meerveld, I., McDonnell, J.J., 2005. The role of lateral pipe flow in hillslope runoff response: an intercomparison of non-linear hillslope response. J. Hydrol. 311, 117–133. https://doi.org/10.1016/j.jhydrol.2005.01.012.

Verdone, M., van Meerveld, I., Massari, C., Penna, D., 2025. Variability and temporal stability of throughfall along a hillslope. J. Hydrol. 647, 132294. https://doi.org/10.1016/j.jhydrol.2024.132294.

Von Freyberg, J., Radny, D., Gall, H.E., Schirmer, M., 2014. Implications of hydrologic connectivity between hillslopes and riparian zones on streamflow composition. J. Contam. Hydrol. 169, 62–74. https://doi.org/10.1016/j.jconhyd.2014.07.005.

Wang, W., Sun, J., Xia, Y., Li, Z., 2023. Identifying hydraulic connectivity among the vadose zone, unconfined and confined aquifers in the thick loess deposits using multiple tracers. J. Hydrol. 626, 130339. https://doi.org/10.1016/j.jhydrol.2023.130339.

Weiler, M., 2017. Macropores and preferential flow—a love-hate relationship. Hydrol. Process. 31, 15–19. https://doi.org/10.1002/hyp.11074.

Weiler, M., McDonnell, J.J., 2007. Conceptualizing lateral preferential flow and flow networks and simulating the effects on gauged and ungauged hillslopes. Water Resour. Res. 43, 1–13. https://doi.org/10.1029/2006WR004867.

Wessolek, G., Schwärzel, K., Greiffenhagen, A., Stoffregen, H., 2008. Percolation characteristics of a water-repellent sandy forest soil. Eur. J. Soil Sci. 59, 14–23. https://doi.org/10.1111/j.1365-2389.2007.00980.x.

Wiekenkamp, I., Huisman, J.A., Bogena, H.R., Lin, H.S., Vereecken, H., 2016. Spatial and temporal occurrence of preferential flow in a forested headwater catchment. J. Hydrol. 534, 139–149. https://doi.org/10.1016/j.jhydrol.2015.12.050.

Williams, M.R., Ford, W.I., Mumbi, R.C.K., 2023. Preferential flow in the shallow vadose zone: effect of rainfall intensity, soil moisture, connectivity, and agricultural management. Hydrol. Process. https://doi.org/10.1002/hyp.15057.

Williams, M.R., Livingston, S.J., Heathman, G.C., McAfee, S.J., 2019. Thresholds for run-off generation in a drained closed depression. Hydrol. Process. 33, 2408–2421. https://doi.org/10.1002/hyp.13477.

Williams, M.R., McAfee, S.J., 2021. Water storage, mixing, and fluxes in tile-drained agricultural fields inferred from stable water isotopes. J. Hydrol. 599, 126347. https://doi.org/10.1016/j.jhydrol.2021.126347.

Worthington, S.R.H., 2019. How preferential flow delivers pre-event groundwater rapidly to streams. Hydrol. Process. 33, 2373–2380. https://doi.org/10.1002/hyp.13520.

Wu, Q., Liu, C., Lin, W., Zhang, M., Wang, G., Zhang, F., 2015. Quantifying the preferential flow by dye tracer in the North China Plain. J. Earth Sci. 26, 435–444. https://doi.org/10.1007/s12583-014-0489-4.

Wuest, S.B., 2009. Comparison of preferential flow paths to bulk soil in a weakly aggregated silt loam soil. Vadose Zo. J. 8, 623–627. https://doi.org/10.2136/vzj2008.0126.

Yan, J., Zhao, W., 2016. Characteristics of preferential flow during simulated rainfall events in an arid region of China. Environ. Earth Sci. 75, 1–12. https://doi.org/10.1007/s12665-015-5101-4.

Zehe, E., Elsenbeer, H., Lindenmaier, F., Schulz, K., Blöschl, G., 2007. Patterns of predictability in hydrological threshold systems. Water Resour. Res. 43, 1–12. https://doi.org/10.1029/2006WR005589.

Zehe, E., Flühler, H., 2001. Preferential transport of isoproturon at a plot scale and a field scale tile-drained site. J. Hydrol. 247, 100–115. https://doi.org/10.1016/S0022-1694(01)00370-5.

Zhang, Y., Tang, Z., Zhang, J., Zhang, Z., Zhang, M., 2024. Visualizing preferential flow paths using dye tracer and species diversity theory methods to explore their correlation to soil properties with random forest algorithm. J. Hydrol. 638, 131570. https://doi.org/10.1016/j.jhydrol.2024.131570.

Zhang, Y., Zhang, Z., Ma, Z., Chen, J., Akbar, J., Zhang, S., Che, C., Zhang, M., Cerdà, A., 2018. A review of preferential water flow in soil science. Can. J. Soil Sci. 98, 604–618. https://doi.org/10.1139/cjss-2018-0046.

Zhu, H., Wang, G., Yinglan, A., Liu, T., 2020. Ecohydrological effects of litter cover on the hillslope-scale infiltration-runoff patterns for layered soil in forest ecosystem. Ecol. Eng. 155. https://doi.org/10.1016/j.ecoleng.2020.105930.